ISTANBUL TECHNICAL UNIVERSITY ★ GRADUATE SCHOOL OF SCIENCE ENGINEERING AND TECHNOLOGY

ANALYSIS OF HISTONE MODIFICATIONS IN FAMILIAL MEDITERRANEAN FEVER PATIENTS USING CHROMATIN IMMUNOPRECIPITATION SEQUENCING ASSAY

M.Sc. THESIS

Begüm FİDAN

Department of Molecular Biology-Genetics and Biotechnology

Molecular Biology-Genetics and Biotechnology Programme

MAY 2015

ISTANBUL TECHNICAL UNIVERSITY ★ GRADUATE SCHOOL OF SCIENCE ENGINEERING AND TECHNOLOGY

ANALYSIS OF HISTONE MODIFICATIONS IN FAMILIAL MEDITERRANEAN FEVER PATIENTS USING CHROMATIN IMMUNOPRECIPITATION SEQUENCING ASSAY

M.Sc. THESIS

Begüm FİDAN
(521111128)

Department of Molecular Biology-Genetics and Biotechnology

Molecular Biology-Genetics and Biotechnology Programme

Thesis Advisor: Assoc. Prof. Dr. Eda TAHİR TURANLI

MAY 2015

İSTANBUL TEKNİK ÜNİVERSİTESİ ★ FEN BİLİMLERİ ENSTİTÜSÜ

AİLESEL AKDENİZ ATEŞİ HASTALARINDA HİSTON MODİFİKASYONLARININ KROMATİN İMMÜNOPRESİPİTASYON DİZİLEME KULLANARAK ANALİZİ

YÜKSEK LİSANS TEZİ

Begüm FİDAN
(521111128)

Moleküler Biyoloji-Genetik ve Biyoteknoloji Anabilim Dalı

Moleküler Biyoloji-Genetik ve Biyoteknoloji Programı

Tez Danışmanı: Doç. Dr. Eda TAHİR TURANLI

MAYIS 2015

Begüm FİDAN, a **M.Sc.** student of ITU **Institute of Science Engineering and Technology** student ID **521111128**, successfully defended the **thesis** entitled "**ANALYSIS OF HISTONE MODIFICATIONS IN FAMILIAL MEDITERRANEAN FEVER PATIENTS USING CHROMATIN IMMUNOPRECIPITATION SEQUENCING ASSAY**", which she prepared after fulfilling the requirements specified in the associated legislations, before the jury whose signatures are below.

Thesis Advisor :	**Assoc. Prof. Dr. Eda TAHİR TURANLI** İstanbul Technical University	.....
Jury Members :	**Assist. Prof. Dr. Aslı KUMBASAR** İstanbul Technical University	.....
	Assist. Prof. Dr. N. C. Tolga EMRE Bogazici University	.....

Date of Submission : 04 May 2015
Date of Defense : 27 May 2015

To my family,

FOREWORD

First and foremost, I would like to express my sincere gratitude to Assoc. Prof. Dr. Eda TAHİR TURANLI for giving me the opportunity to be a member of her lab, her supervison, help, advice and support.

I wish to thank to a number of individuals for contribution to this project. In particular, I would like to thank Assist. Prof. Dr. N. C. Tolga EMRE for giving the opportunity to monitoring their ChIP experiments and advices. Thanks to İlker KARACAN and Can KÜÇÜK for providing advice with the bioinformatic analysis. Thanks to Assoc. Prof. Dr. Serdal UĞURLU and Dilşen ÇEVİRGEN for the processing the patient samples. Thanks to Biopolymers Facility for performing the ChIP-Seq experiment. Thank to all patients and healthy volunteers.

I am also thankful to Gökçe ÇELİKYAPI ERDEM, Aslı KİREÇTEPE AYDIN, Timuçin AVŞAR, Ayşe ERÖZENCİ and Şule ERDEMİR for their guidance and help. I am also very grateful to Elif EVEREST, Pelinsu KÖPRÜLÜ, Neslihan SEVİNÇ, Ayşe BALAMİR, Gila BENYAKAR and to my other colleagues for their patience and scientific support.

My biggest thanks to Caner YILDIRIM for always being there to encouragement and support me.

Lastly, I want to expess my deeply thanks to my dearest family, my father Halil FİDAN, my mother Serap FİDAN and my brother Burak FİDAN for their endless love, patience and support.

May 2015

Begüm FİDAN
(Molecular Biologist)

TABLE OF CONTENTS

Page

ABBREVIATIONS

˚C	**:** Degrees Celsius
5mC	**:** 5-methylcytosine
5hmC	**:** 5 hydroxymethyl cytosine
C5	**:** Carbon-5
AS	**:** Alternative splicing
Bp	**:** Base pair(s)
CG	**:** Cytosine-guanine
ChIP	**:** Chromatin immunoprecipitation
ChIP-Seq	**:** ChIP-Sequencing
CLB	**:** Cell lysis buffer
CpG	**:** Cytosine-phosphate-guanine
Ct	**:** Threshold cycle
DMSO	**:** Dimethyl sulfoxide
DNA	**:** Deoksiribonucleic acid
DNMT	**:** DNA methyltransferase
dNTP	**:** Deoxyribonucleotide triphoshphate
EDTA	**:** Ethylenediaminetetraacetic acid
FDR	**:** False discovery rate
Fl	**:** Full length
FMF	**:** Familial Mediterranean Fever
g	**:** Grams
g	**:** Centrifugal force
GAPDH	**:** Glyceraldehyde 3-phosphate dehydrogenase
GO	**:** Gene ontology
H3	**:** Histone 3
Hr	**:** Hour(s)
HAT	**:** Histone acetyltransferase
HDAC	**:** Histone deacetylase
HDMs	**:** Histone demethylase
HL-60	**:** Human promyelocytic leukemia cells
HMTs	**:** Histone methyltransferases
IP	**:** Immunoprecipitation
IgG	**:** Immunoglobulin G
IL-1β	**:** Interleukin 1β
K	**:** Lysine
KATs	**:** Lysine acetyltransferases
Kb	**:** Kilobase
LPS	**:** Lipopolysaccharide
M	**:** Molar
MACS	**:** Model-based Analysis of ChIP-Seq
Mb	**:** Megabase pair(s)
mL	**:** Mililiter(s)
MBD	**:** Methyl-CpG-binding domain
me	**:** Methylation

MeCP2 : Methyl-CpG-binding protein 2
MEFV : MEditerranean FeVer
mg : Milligram(s)
Min : Minutes
mL : Milliliter(s)
mM : Millimolar
mRNA : Messenger RNA
N-terminal : Amino terminal
N-ChIP : Native ChIP
Ng : Nanogram(s)
NGS : Next generation sequencing
Nm : Nanometre
nM : Nanomolar
ORF : Open reading frame
PBMCs : Peripheral blood mononuclear cells
PBS : Phosphate buffer saline
PBS-T : PBS-Tween 20
PCR : Polymerase chain reaction
PIC II : Protease Inhibitor Cocktail II
P/M : Pyrin/marenostrin
PMNs : Polymorphonuclear cells
PRYSPRY : B30.2 Domain
PSTPIP1 : Proline Serine Threonine Phosphatase-Interacting Protein 1
PTMs : Post-translational modifications
QC : Quality control
ORF : Open reading frame
qPCR : Quantitative PCR
RNA Pol II : RNA polymerase II
RNase A : Ribonuclease A
rpm : Rounds per minute
RT-PCR : Real time-PCR
SAM : S-adenosyl methionine
SDS : Sodium dodecyl sulfate
SDS-PAGE : Sodium Dodecyl Sulfate-Polyacrylamide Gel Electrophoresis
SE : Single end
Sec : Seconds
SICER : Statistical approach for the Identification of ChIP-Enriched Regions
SNP : Single nucleotide polymorphism
TAE : Tris-acetate-EDTA
TE : Tris-EDTA buffer
TTS : Transcription termination site
TSS : Transcription start site
UHRF1 : Ubiquitin-like with PHD and ring finger domains 1
UTR : Untranslated region
UV : Ultraviolet
V : Volt
µg : Microgram
µL : Microliter
µM : Micromolar
X-ChIP : Crosslinked ChIP

LIST OF TABLES

Page

LIST OF FIGURES

Page

ANALYSIS OF HISTONE MODIFICATIONS IN FAMILIAL MEDITERRANEAN FEVER PATIENTS USING CHROMATIN IMMUNOPRECIPITATION SEQUENCING ASSAY

SUMMARY

Familial Mediterranean Fever (FMF) is mainly an autosomal recessive inherited disease affects mostly Jewish, Arab, Turk and Armenian populations and characterized by irregular inflammatory attacks of fever. FMF responsible gene is MEFV which localizes on short arm of chromosome 16 and consists of 10 exons that comprise a 3,7 kb transcript. The protein encoded by MEFV is Pyrin/Marenostrin (P/M) that 781 amino acid protein, 86 kd moleculer weight and localizes in cytoplasm. More than 200 mutations/variations were detected in MEFV gene which mostly localize on exon 2 and exon 10 until now. The most common five of these mutations are M694V, M694I, V726A, M680I and E148Q. While 80% of FMF patients carry mutation in MEFV, 15-20% of patients carry no mutations in the gene.

Our previous studies showed a possibility of epigenetic regulation in this disease development, based on finding of increased exon methylation at exon 2 (p=0.049), reduced gene expression and increased exon 2 deleted transcript splice form of MEFV gene (p=0.026) compared to healthy controls.

Epigenetics is the study of changes in gene expression wtihout changes in deoksiribonucleic acid (DNA) sequence. These changes are controlled by three major mechanisms which are DNA methylation, histone modifications and RNA associated silencing. DNA methylation and histone modifications do not act independently from each other. DNA is packaged by histone proteins, other proteins and RNA into chromatin. Nucleosome that is the basic unit of chromatin, consist of ~147 bp of DNA tightly wrapped around the histone octamer which include two copies of H2A, H2B, H3, and H4 proteins. Through post-translational modifications of histone tails mostly, chromatin structure can be either condensed or open. These modifications are potentially reversible and heritable. Post-translational modifications of N-terminal of histones include acetylation, methylation, ubiquitylation and sumoylation of lysine residues, methylation of arginine residues, phosphorylation of serine and threonine residues. Histone lysine methylations can be associated with transcriptional activation, such as trimethylations of Histone 3 lysine 4 (H3K4me3) and repression, such as trimethylations of Histone 3 lysine 9 (H3K9me3), commonly referred to as euchromatin and heterochromatin modifications, respectively. The reversible modifications of histones affect the histone-histone and histone-DNA interactions and thus regulate the chromosome structure and gene expression.

In the light of all, we were performed chromatin immunoprecpitation (ChIP) followed by qPCR confirmation and high throughput sequencing (ChIP-Seq) for genome wide analysis of variations in methylated histones (H3K9me3 and H3K4me3) in peripheral blood mononuclear cells (PBMCs) from 10 FMF patients during attack period, the same 10 FMF patients during attack-free period and 10 healthy subjects to assess whether the modifications are related to inflammation and

analyse the chromatin dynamics of FMF patients. ChIP-Seq data was generated (177,447,268 bases) from Illimuna HiSeq 2500 and examined with bioinformatic analysis. Firstly, ChIP-Seq data were converted to fastqsanger format and uniquely aligned to reference genome (human, hg19) after quality control. Then, significantly enriched regions were detected by peak callers which are MACS and SICER (FDR<0.01). Then, peaks were annotated in the human reference genome and visualised by IGV and UCSC Genome Browsers. Bioinformatic analysis revealed H3K4me3 modification regions nearly 10 fold enriched than H3K9me3 modifications throughout the genome in all study groups. We found a significant enrichment of H3K4me3 in the candidate genes in FMF patients during attack period. Furthermore, H3K4me3 peaks were observed in mostly regulatory regions of some inflammation related and pyrin inflammation pathway associated genes which included MEFV gene region. Then, ChIP-Seq results were confirmed using MEFV primers amplifying MEFV promoter and exon 1 regions which are represented to predetected peak region, GAPDH primers as a housekeeping control and negative control primers by polymerase chain reaction (PCR). Enrichment of H3K4me3 in several autoinflammatory disease-related genes and MEFV (p-value=$1.39x10^{-8}$, fold change=3.4, FDR=$1.77x10^{-8)}$ suggests that epigenetic modifications may have a role in progression of inflammation in FMF patients, which require further analysis.

For future studies, a larger number of patients and control sapmles are needed for statistical analysis and validation of the ChIP experiment. ChIP-Seq data can be confirmed by quantitative real time PCR (qPCR). In addition to ChIP experiment, it should be coupled with high throughput sequencing which will be generated with high coverage for each sample in order to deeper genome wide analysis of the histone modifications. Also, different histone modifications should be analysed with more precise method, coupled with DNA methylation and alternative splicing studies for deeper understanding of the epigenetic status of the FMF disease.

AİLESEL AKDENİZ ATEŞİ HASTALARINDA HİSTON MODİFİKASYONLARININ KROMATİN İMMÜNOPRESİPİTASYON DİZİLEME KULLANARAK ANALİZİ

ÖZET

Ailesel Akdeniz Ateşi (AAA) büyük çoğunlukla Türk, Ermeni, Yahudi ve Arap gibi Akdeniz kökenli toplumlarda görülen otoinflamatuar bir hastalıktır. Türkiye'de yaygınlığı 1:1000 ve yaygınlık frekansı 1:5'dir. AAA periton, plevra ya da sinovyum seröz membranlarından birinde oluşan inflamasyonun neden olduğu iltihap sonucu ortaya çıkan yüksek ateşle (38,5-40˚C) birlikte ciddi karın, göğüs ve eklem ağrılarının eşlik ettiği ani ve düzensiz ataklarla birlikte seyreder. Ataklar genellikle 1-3 gün boyunca sürer. Hastaların 70%'inde hastalık belirtileri ilk 10 yılda ortaya çıkar ve 90%'nında ise ilk 20 yılda hastalık başlangıç gösterir. Atak bölgeleri ve şiddeti bir hasta için farklılık gösterebileceği gibi her hasta için de farklı olabilmektedir.

Klinik tanıda yüksek ateş, karın ağrısı, göğüs ağrısı ve hastanın Kolşisin ilacına verdiği cevap dikkate alınır. 1972 yılından beri hastalığın tedavisinde kolşisin ilacı kullanılır. Tedavi düzenli ve uzun süreli olmalıdır. Hastaların 90%'nında yeterli dozda ve düzenli olarak kullanıldığında atakların tamamen düzeldiği, 30%'unda ise atakların şiddeti ve sıklığının azaldığı, 5%'inde ise bu ilaca yanıt vermediği gözlenmiştir. Kolşisin tedavisine cevap vermeyen hastalarda amiloidoz birikimi riski çok yüksektir. Amiloidoz, başta böbrek olmak üzere diğer organlarda fonksiyon bozukluğu veya yetersizliğe yol açan suda erimeyen bir proteinin gelişimiyle ortaya çıkan bir hastalıktır. Klinik tanıda idrar testlerinin yapılması amiloidoz varlığının tespitinde önemli yer tutar. Hastalığa kesin tanı koyacak bir laboratuar testi yoktur. Atak döneminde bazı laboratuar bulguları anormal olarak tespit edilebilir ancak hiç biri tanı koymaya yeterli değildir. AAA'nde görülen klinik bulgular pek çok hastalıkta da görülebildiği için hastalığın tanısı çoğu zaman gecikebilmektedir. Aile geçmişinde AAA hastalığı olan, klinik bulguları ve etnik yapısı uygun olan kişilerde tanının kesinleşmesi için genetik test yapılabilir. Ancak unutulmamalıdır ki genetik testi pozitif olanların hepsi AAA olmadığı gibi, negatif olanlar da AAA olabilir.

AAA otozomal resesif (çekinik) geçiş gösteren kalıtsal bir hastalıktır. Yani hastalığın ortaya çıkması için anne ve/veya babanın bu hastalık genlerini taşıması gerekir. Stres, enfeksiyon, aşırı fiziksel egzersiz, yorgunluk, travma gibi tetikleyici çevresel etkenlerin dışında MEFV geninde meydana gelen mutasyonlar AAA'ne yol açar. MEFV geni 1992'de haritalanmış ve 1997'de ise klonlanmıştır. MEFV 16. kromozomun kısa kolu üzerinde (16p13.3 noktasında) yerleşim gösterir ve 10 ekzondan oluşur. MEFV geni 781 amino asitten oluşur ve pyrin/marenostrin adı verilen bir proteini kodlamaktadır. Bu proteinin fonksiyonu tam olarak bilinmemekle birlikte inflamasyon kontrolünde rol oynadığı ve özellikle nötrofillerde ifade olduğu ileri sürülmektedir.

Şimdiye kadar MEFV geni üzerinde büyük çoğunluğunu yanlış anlamlı (missense) mutasyonların oluşturduğu amino asit dizisinde değişikliğe yol açan ve proteinin yapısını ve fonksiyonunu bozan 200'den fazla mutasyon/varyasyon tespit edilmiştir. Bu mutasyonlardan en sık görülen 5 tanesi M694V, M694I, M680I, E148Q, V726A'dır ve ekzon 2 ve ekzon 10 üzerinde meydana gelirler. MEFV mutasyonların çoğu 10. ekzon üzerinde birikmiştir ve pyrin proteinin PRYSPRY alanı tarafından kodlanmaktadırlar. Bunun dışında çoğu nadir görülen mutasyonlar 2. ve 5. ekzonlarda yoğunlaşmışlardır ve pyrin proteini'nin bu mutasyonlar üzerine etkisi henüz bilinmemektedir.

MEFV geni 3700 baz çiftlik (bç) bir mRNA kodlamaktadır. Bu gen genellikle nötrofiller, eozinofiller, sitokin aktive monositler, dendritik hücreler ve sinovyal fibroblastlarda ifade edilir fakat lenfositlerde ifade edilmez. FMF hastalarının atak döneminde polimorfik nükleer hücrelerde anormal trafik ve ataksız döneminde MEFV mRNA ifadesinin periferik kandaki löksitlerde azaldığı tespit edilmiştir. MEFV mRNA çoğunlukla 2., 3., 4. ve 8. ekzonu içeren alternatif birleşmeye maruz kalmaktadır. En az 16 tane farklı mRNA formu tespit edilmiştir: tam boy, MEFV-d2 (2 Δ), ekzon 2a (2a), ekzon 4a (4a), ekzon 8ext (8ext), Δ2/4a, 2a/4a, Δ2/8ext, 2a/8ext, del234, del2345, del34, del7, del78, 9ext and 2Δ /9ext. MEFV geninin tam boy kopyası olan pyrin proteini sitoplazmik bölgede yerleşim gösterirken, 2. ekzonu içermeyen alternatif kopyasının ise nükleusta yerleşim gösterdiği tespit edilmiştir. Ayrıca bu formun AAA hastalarında sağlıklı gruba oranla daha çok kodlandığını daha önceki çalışmalarımızda gösterilmiştir.

MEFV genindeki genetik değişikliklerin yanı sıra pek çok epigenetik olay AAA hastalığının ortaya çıkmasında rol oynamaktadır. Epigenetik, DNA dizisi üzerinde bir değişiklikle meydana gelmeden ancak gen ifadesinde değişikliğe yol açan yani kalıtsal olan fenotipik değişiklikleri inceler. 3 temel epigenetik mekanızma; DNA metilasyonu, histon modifikasyonları ve RNA alternatif kırpılmalarıdır. Epigenetik mekanizmalar gen ifadesini dolaylı veya doğrudan etkilemesine bağlı olarak ikiye ayrılır. Post-translasyonel yani DNA'nın mRNA'yı kodladıktan sonra meydana gelen değişiklikler gen ifadesini dolaylı olarak etkilerler. DNA ve kromatin boyutundaki modifikasyonlar ise doğrudan gen ifadesini etkilerler.

DNA düzeyindeki en bilinen modifikasyon DNA metilasyonudur ve DNA-protein etkilşimini yöneterek gen ekspresyonunu kontrol eder. DNA metilasyonu genellikle sitozin ve guanin bazlarından zengin olan ve CpG adacığı olarak adlandırılan bölgede, sitozin bazının 5. karbonu üzerine metil grubunun bağlanması ile meydana gelir. DNA metillenmesinde S-adenozil metiyonin (SAM) metil donörü olarak işlev görür ve DNA metiltransferaz enzimi reaksiyonu katalizler. Metillenen DNA sıkı bir yapılanma gösterirken (heterokromatin), metillenmemiş bölgeler daha serbest bir şekilde (ökromatin) paketlenirler. Laboratuar grubumuz daha önceki çalışmalarda MEFV geninin 2. ekzonu üzerindeki DNA metilasyonun AAA hastalarında sağlıklılara oranla daha yüksek olduğunu tayin etmiş ($p=0.049$) ve böylece DNA metilasyonu ile AAA ile ilişkisini göstermişlerdir.

Kromatin boyutundaki modifikasyonlar kovalent ve nonkovalent olmak üzere ikiye ayrılırlar. Kovalent modifikasyonlar histon modifikasyonlarıdır. DNA, histon proteinler, diğer proteinler ve RNA ile birlikte paketlenerek kromatin ipliğini oluşturur. Yaklaşık 147 baz uzunluğundaki negatif yüklü DNA pozitif yüklü histon proteinlerine bağlanmak ve etrafında 2 defa dönmek suretiyle histon oktomerine (H2A, H2B, H3 ve H4 proteinlerinin ikişer kopyasından oluşur) bağlanır ve

kromatinin temel yapısı olan nükleozomu oluşturur. DNA histon proteinlerine bağlanarak açık (ökromatin) veya kapalı (heterokromatin) bölgeleri oluşturur. Post-translasyonel histon modifikasyonları gen ifadesini etkileyen önemli epigenetik bir mekanizmadır. Histon kuyruklarının amino uçları lizin rezidülerinin asetilasyonu, metilasyonu, fosforilasyonu, übikitinasyon, sümoylasyonu, arjinin rezidüleri metilasyonu, serin ve treonin rezidülerinin fosforilasyonu gibi çok sayıda modifikasyona maruz kalır. Tersinir post-translasyonel histon modifikasyonları histon-histon ve histon-DNA etkileşimini dolayısıyla kromatin yapısını ve o geni açık veya kapalı duruma getirerek gen ekspresyonunun gerçekleşip gerçekleşmeyeceğini belirlerler. Histon kuyruğuna asetil grubunun bağlanmasıyla DNA serbest yapıya ulaşır ve gen ifadesi gerçekleşir. Asetil grubunun bağlanmasından histon asetil transferaz (HAT), ayrılmasında ise histon deasetil transferaz (HDAT) enzimi sorumludur. Diğer bir post-translasyonel modifikasyon olan histon metilasyonu yerleşimine bağlı olarak aktif veya pasif kromatinin belirleyicisi olabilir.

Histon metilasyonu, histon proteinlerinde bulunan amino asitlere (lizin, arjinin, serin, treonin) histon metil transferaz (HMT) enzimleri tarafından 1, 2 veya 3 metil grubunun eklenmesiyle meydana gelir. Histon lizin metilasyonu aktif transkripsiyon ile ilişkili olabileceği gibi (örneğin Histone H3 lizin 4 (H3K4), Histone H3 lizin 36 (H3K36)), pasif transkripsiyon ile de (örneğin Histone H3 lizin 9 (H3K9), Histone H3 lizin 27 (H3K27)) ilişkili olabilir. H3K9me3 histon modifikasyonu genellikle gen susturulmasında rol oynar ve heterokromatin bölge ile ilişkilidir. H3K4me3 modifikasyonu ise aktif gen bölgelerini temsil eder ve ökromatin ile ilişkilidir. Tüm genom boyu yapılan çalışmalar H3K4me3 modifikasyonunun genellikle CpG adacığının yer aldığı promoter ve transkripsiyon başlangıç bölgesinde bulunduğunu ifade etmektedir. İki önemli epigenetik mekanizmanın, DNA metilasyonu ve kromatin modifikasyonu, birbirlerinden tamamen bağımsız olmadığı yapılan çalışmalarda gösterilmiştir.

Bu çalışmanın odak noktası AAA hastalarında H3K9me3 ve H3K4me3 modifikasyonlarının tüm genom boyunca dağılımlarının yanı sıra MEFV geni üzerindeki DNA metilasyonu ve inflamasyon ile ilişkilerini analiz etmektir. 10 AAA hastasının atak ve ataksız dönemlerinde (4 kadın, 6 erkek) ve 10 sağlıklı (5 kadın, 5 erkek) bireylerinden elde edilen periferik tek nükleuslu hücreler ile hedef proteine spresifik antikorlar kullanılarak kromatin immünopresipitasyon (ChIP) analizini takiben polimeraz zincir reaksiyonu (PZR) ile ChIP doğrulandı ve yeni nesil dizileme ile birleştirildi. Metillenmiş H3K9(me3) ve H3K4(me3)'ün genom boyunca dağılımları dizileme sonuçları kullanılarak biyoinformatik analiz ile değerlendirildi.

Öncelikle tüm bireylerden MEFV ekspresyonun var olduğu periferik kan tek nükleuslu hücreler yoğunluk farkı methodu ile izole edilmiştir. Formaldehit ile proteinler DNA'ya bağlanmış ve glisin solüsyonu ile bağlanma işlemi sonlandırılmıştır. PBS çözeltisi ile yıkanan hücreler formaldehitten uzaklaştırıldıktan sonra liziz buffer ile hücreler patlatılmış ve içeriği ortaya çıkartılmıştır. Sonikasyon ile proteinlere zarar vermeden kromatinler ortalamaları 500 baz olmak üzere 200 - 700 baz aralığında küçük parçalara ayrılmıştır. İmmünopresipitasyon aşamasında hedef modifikasyonlara spesifik antikorlar öncelikle manyetik boncuklara bağlanmış ve daha sonra elde edilen kompleks hücre lizatı ile inkübe edilerek immün kompleks oluşturulmuştur. Hücre lizatının bir kısmı input olarak daha sonraki aşamalarda kullanılmak üzere saklanmıştır. Seri yıkamaların ardından immün kompleks ve input kontrol yüksek sıcaklığa maruz bırakılarak protein/DNA çapraz bağları tersine

çevrilmiş ve protein, RNA gibi içerikler uzaklaştırıldıktan sonra saf DNA izole edilmiştir. Elde edilen DNA modifikasyonlara spesifik antikorların bağlandığı bölgeleri temsil etmektedir ve analizleri için kromatin immünopresipitasyon yeni nesil dizileme ile birleştirilmiştir. Dizileme sonucu elde edilen 50 bazlık kısa okumalar referans genoma (hg19) haritalanmış ve okumaların yarısından fazlasının genomun tek bir bölgesi ile spesifik olarak eşleştiği tespit edilmiştir. Okumaların yoğunlaştığı bölgeler pikler ile hizalanmış ve bu aşamada kontrol olarak input kullanılmıştır (Mfold=32). Bu piklerin temsil ettiği genler tespit edilmiş ve yerleşimleri görüntülenmiştir. Biyoinformatik analiz, tüm çalışma gruplarında inaktif transkripsiyonu temsil eden H3K9me3 modifikasyonunun genom boyunca dağılımının aktif transkripsiyonu temsil eden H3K4me3 modifikasyonundan yaklaşık 10 kat daha az olduğunu yansıtmaktadır. H3K4me3 modifikasyonlarının coğunlukla genin düzenleyici bölgelerinde ve H3K9me3 modifikasyonlarının ise intragenik bölgelerde yerleştikleri tespit edilmiştir. Ayrıca, her iki modifikasyona ait okumaların tüm çalışma grubuna ait örneklerde MEFV geni ile eşleştiği tespit edilirken H3K4me3 modifikasyonuna ait okumaların atak dönemdeki AAA hastalarında MEFV genin promoter, 1. ekzon ve 1. intron'un bir kısmını kapsayan bölgesinde ataksız dönemdeki AAA hastaları ve sağlıklı kontrollere göre çok daha fazla yoğunlaştığı tespit edilmiştir. Bunun yanında H3K4me3 modifikasyonunun otoinflamasyonda rol oynayan ve pyrin proteini ile ilişkili bazı genlerin çoğunlukla promoter bölgelerinde ataklı AAA hastalarında, sağlıklı ve ataksız AAA hastalarından daha fazla bulunduğu tespit edilmiştir. Biyoinformatik analiz sonucu PZR kullanılarak MEFV geninde tespit edilen pik bölgesini çoğaltan 2 ayrı PZR ve GAPDH pozitif kontrol primerleri kullanılarak doğrulanmıştır. Bu sonuç H3K4me3 modifikasyonunun AAA hastalarında DNA metilasyonu ve inflamasyon ile ilişkisi olabileceğini düşündürmektedir.

Gelecekte yapılacak çalışmalarda istatistiksel analiz ve ChIP doğrulaması için daha kontrol ve hasta gruplarına ait fazla sayıda örnek kullanılmalıdır. ChIP-Seq sonucu belirlenen aday gen bölgeleri qPCR ile doğrulanmalıdır. Yeni nesil dizilemeden daha fazla okuma sayısı elde edebilmek için, dizileme tekrarlanmalı ve böylece histon modifikasyonlarının tüm genom boyunca dağılımları daha derinlemesine incelenmiş olacaktır. ChIP, ilişkili olabilecek diğer histon modifikasyonlarına spesifik antikorlar ile tekrarlanmalı ve DNA metilasyonu, alternatif kırpılmış formların analiz çalışmaları ile birleştirilmelidir. Böylece AAA hastalığının patolojisinin ve epigenetik mekanizması daha derinlemesine anlaşılabilmesine yardımcı olacaktır.

1. INTRODUCTION

1.1 Familial Mediterranean Fever Disease and MEFV Gene

Familial Mediterranean Fever (FMF) is the most common autoinflammatory disease which affects primarily people of Mediterranean area such as Jewish, Arab, Turkish and Armenian populations. Prevalance of FMF in these populations is estimated as 1:200 to 4:1000 (Akpolat et al., 2012; Bonyadi et al., 2015; Ahmadinejad et al., 2014).

FMF is characterized by spontaneous and irregular inflammatory attacks of fever (38,5-40°C), accompanied by serositis, synovitis and subclinical chronic inflammatory state, resulting in for example anemia and splenomegaly. Also, abdominal pain occurs in 95% of the patients (Berkun et al., 2011; Ben-Zvi et al., 2012; De Jesus and Mansky, 2013; Federici et al., 2012). Most attacks generally lasts from 12 to 72 hours and occurs every few weeks to months. Patients are normally asymptomatic between attacks, but subclinical inflammation may persist (Chae et al., 2009). Salient features of a typical attack are abdominal pain, pleurisy, arthritis (usually monoarticular), rash, febrile myalgia, neutrophilia and acute phase response (Galon et al., 2000).

FMF-associated inflammatory (or AA) amyloidosis occurs in some patients with severe inflammatory attacks beginning early in life which can leads to kidney failure and death, whereas may infrequently occur even in patients with no recognised clinical inflammatory crisis (Federici et al., 2012). Furthermore, in most patients, the onset of disease begins before the age of 20 years (Galon et al., 2000). The prevalence of amyloidosis varies according to ethnic groups, suggesting that genetic and/or environmental factors join the genesis of amyloidosis in FMF (Federici et al., 2012).

Clinical diagnosis of FMF include frequent symptoms such as abdominal and thoracic pain, family history and response to treatment with colchicine drug. Nonetheless, mutations analysis in MEFV gene is essential for a definitive FMF

diagnosis. But, about 25% of the FMF patients carry one mutation and 10-15% carry no mutation in MEFV gene. So, the clinical diagnosis of FMF still important (Ben-Zvi et al., 2015). Treatment of FMF daily and for a long time with colchicine that is known to target microtubules, prevent attacks and formation of amyloidosis. Starting dose may be increased from 1 mg/day to 1,5 to 2 mg/day according to weight or body surface area (De Jesus and Mansky, 2013; Ahmadinejad et al., 2014; Federici et al., 2012). Although, colchicine mechanism is not clear, it may be a results of the inhibition of the inflammasome or the inhibition of the migration of inflammatory cells in inflamed tissues. Nevertheless, some patients are not sensitive to colchicine (Ozkurede and Franchi, 2012).

Missense mutation in the MEFV (MEditerranean FeVer) gene results in FMF that is an autosomal recessive disorder via a defect in the product of protein and onset of inflammatory cycle. Morever, environmental factors such as emotional stress, infection, extreme physical exercise, fatigue, trauma and menses can be trigger factors (Centola et al., 2000; Ahmadinejad et al., 2014). MEFV gene associated with FMF was mapped to the short arm of chromosome 16 in 1992 and cloned in 1997 (Federici et al., 2012). The gene is located in 16p13.3 and consist of 10 exons that comprise a 3,7 kilobase (kb) transcript (Touitou, 2001; Diaz et al., 2004). MEFV gene is mostly expressed in neutrophils, eosinophils, cytokine activated monocytes, dendritic cells and synovial fibroblasts (Kirectepe et al., 2001). The protein encoded by MEFV is pyrin (or marenostrin) that is a 781 amino acid protein, 86 kilodalton moleculer weight (Touitou, 2001; Booty et al., 2009). The expression of MEFV is increased by interferon γ (IFN-γ), tumor necrosis factor α (TNF-α), lipopolysaccharide (LPS) and interleukin 1β (IL-1β) which are proinflammatory agents (Touitou, 2001).

1.2 The MEFV Gene and Its Expression

1.2.1 MEFV variations

Until now more than 200 FMF-associated variations in MEFV have been reported in the Infevers registry (Menthie`re, 2003). The majority of mutations are missense changes localized on exons 2 and 10 (Grandemange et al., 2009). Five of these mutations (M694V, M694I, V726A, M680I in exon 10 and E148Q in exon 2) were usually found in the mainly affected populations (Hashim, 2010; Booty et al., 2009).

Structure of the MEFV gene and localization of common mutations on the gene shown in Figure 1.1.

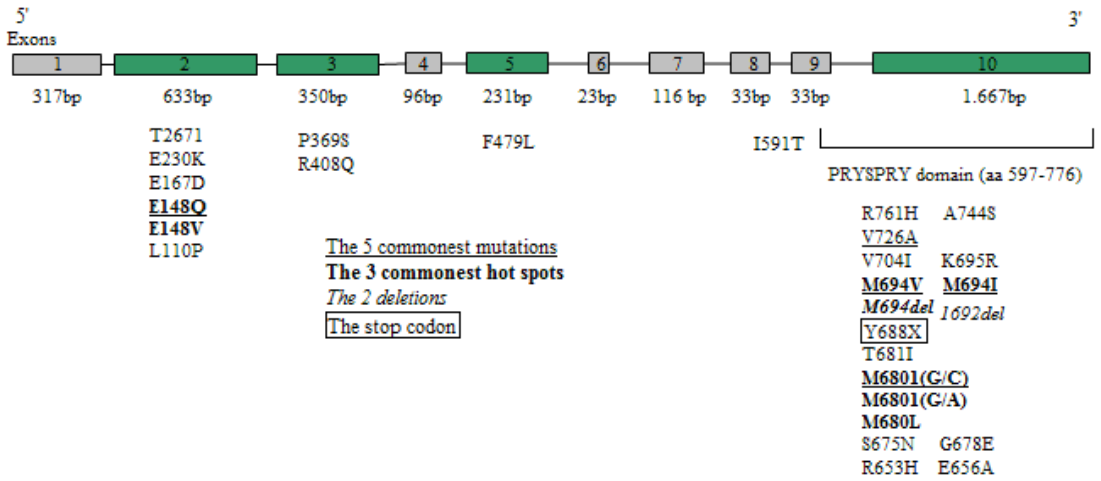

Figure 1.1: Structure of the MEFV gene and localization of common mutations on the gene, adopted from (Touitou, 2001).

Most FMF-associated mutations are single amino acid substitutions (missense mutations), and a few single amino acid duplication/deletion mutations have also been reported. Only two mutations, a frame-shift in exon 2 and a nonsense mutation in exon 10, have been reported to produce truncated proteins. At a molecular level, FMF-associated pyrin mutations might lead to a gain of function, with gene dosage effect, rather than a loss of function, as would be expected for more straight forward recessive diseases (Chae et al., 2009).

The greater number of MEFV mutations are accumulated in exon 10, which encodes the carboxy-terminal B30.2 (or PRYSPRY) domain. Structure of the SPRY domain suggests that at least some of the pyrin mutations map to the loop regions of the beta-sandwich structure and may disrupt a SPRY domain–mediated protein–protein interaction, including an interaction with caspase 1 (Üstek et al., 2007). Also, significant number of rare mutations cluster in exons 2 and 5; however, the effect of these variants on the function of pyrin is unknown (The International FMF Consortium, 1996).

Some mutations are more pathogenic than others, yet clinical expression of the disease can vary among patients having the same mutations (Ece et al., 2014). Homozygosity for M694V, the most frequent mutation, is associated with a severe form of FMF, whereas homozygosity for E148Q is associated with mild disease expression and low penetrance (Notarnicola et al., 2002). Types of MEFV mutations

and clinical picture of FMF alteration in different geographic regions and ethnic groups (Ece et al., 2014).

Furthermore, MEFV mutations are thought to be also involved in non-FMF conditions, such as Behçet Disease (Livneh et al., 2001; Touitou et al., 2000), Rheumatoid Arthritis (RA) (Touitou, 2001), Ankylosing Spondylitis (AS) (Cosan et al., 2010), Crohn's Disease (CD) (Fidder et al., 2005) and recently abdominal pain (Touitou, 2001). Also, some polyfactorial inflammatory disease are more common in FMF patients than in the ethnically matched general population such as Inflammatory Bowel Disease (Cattan et al., 2000) and Behçet Disease (Touitou, 2001). These evidence have been suggest that MEFV may be general inflammatory response gene rather than specific only for FMF disease.

1.2.2 MEFV gene expression regulation

MEFV is expressed predominantly in neutrophils, eosinophils and monocytes but not in lymphocytes (Centola et al., 2000). MEFV is also expressed in dendritic cells and synovial fibroblasts (Diaz et al., 2004). In monocytes, the expression levels are variable and the expression is up-regulated by proinflammatory agents, such as interferon-c (IFN-c), TNF- α and LPS. However, the monocytic cell lines U937 and THP-1 also express MEFV, the promyelocytic cell line human promyelocytic leukemia cells (HL-60) expresses MEFV only after granulocytic and monocytic differentiation. MEFV expression is observed at the myelocyte stage during granulocyte differentiation in CD34+ hematopoietic stem-cells (Chae et al., 2009). MEFV expression is also observed in fibroblasts from synovium, peritoneum, and skin at a lower level compared to neutrophils, and the expression is increased by IL-1β or phorbol myristate acetate (Matzner et al., 2010).

Human MEFV messenger RNA (mRNA) is expressed in polymorphonuclear cells (PMNs), eosinophils and monocytes, but absent from lymphocytes. It is probable that FMF attacks reflect abnormal trafficking of PMNs or altered chemotactic signaling from monocyte/macrophages (Diaz et al., 2004). During attack-free periods, expression of MEFV mRNA reduce in peripheral blood leukocytes (PBLs) in FMF patients (Üstek et al., 2007).

The MEFV pre-mRNA is subject to alternative splicing. MEFV gene has lots of alternatively-spliced transcripts, but five major splicing events involving exons 2, 3,

4 or 8 (Grandemange et al., 2009). There are at least 16 MEFV spliced-isoforms: full-length (fl), MEFV-d2 (2 Δ), exon 2a (2a), exon 4a (4a), exon 8ext (8ext), Δ2/4a, 2a/4a, Δ2/8ext, 2a/8ext, del234, del2345, del34, del7, del78, 9ext and 2Δ /9ext. Among these MEFV alternative transcripts only seven transcripts can be translated to proteins: Full length (fl), 2a, 2 Δ, 8ext, 2Δ /8ext, 2Δ /9ext and 2a/4a; although other transcripts are degraded by nonsensemediated decay (Hashim et al., 2010; Diaz et al., 2004; Grandemange et al., 2009). Previous studies showed a increased exon 2 deleted transcript splice form of MEFV gene in FMF patients compared to healthy control (p=0.026) (Kirectepe et al., 2011b).

1.3 MEFV Protein: PYRIN/MARENOSTRIN

Pyrin/marenostrin (P/M) is encoded by the MEFV locus, and localizes in the cytoplasmic perinuclear area. The role of P/M appears to be in the regulation of inflammation at the level of leukocyte cytoskeletal organization (Notarnicola et al., 2002; Chae et al., 2009). Full-length pyrin exclusively localizes to the cytoplasm, while a rare isoform encoded by transcripts lacking exon 2 can enter the nucleus rather than cytoplasm (Chae et al., 2009). However, endogenous pyrin is predominantly localized to the nucleus in synovial fibroblasts, dendritic cells, and polymorphonuclear cells, but to the cytoplasm in monocytes (Diaz et al., 2009).

Pyrin is composed of five different domains: (i) a PYRIN domain; (ii) a bZIP transcription factor basic domain; (iii) a B-box zinc finger domain; (iv) an a-helical (coiled-coil) domain; (v) a B30.2 (PRYSPRY) domain (Figure 1.3). Each domain has a distinctve role in interactions with proteins that are related to inflammation through regulation of cell death, cytokine secretion, transcriptional regulation, and cytoskeletal signalling. The identification of multiple binding partners suggests that pyrin participates in several molecular pathways (Chae et al., 2009).

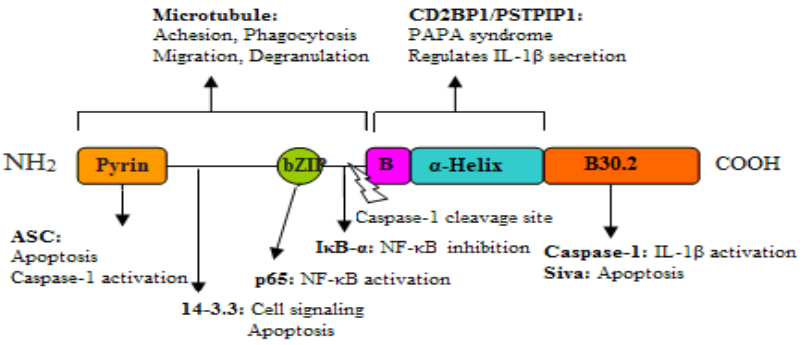

Figure 1.2: Structure of pyrin/ marenostrin protein, adopted from (Chae et al., 2009).

P/M interacts with several cellular proteins, including the adaptor protein ASC, Proline Serine Threonine Phosphatase-Interacting Protein 1 (PSTPIP1) and Siva. ASC is an adaptor protein that is an important component of both the apoptosome and the inflammasome. ASC responsible for mediating proteolytic activation of procaspase-1 into caspase-1 via PYD-PYD interaction (Taskiran et al., 2012; Grandemange et al., 2009). PSTPIP1 is a cytosolic adaptor protein that functions to link PEST phosphatases to their substrates. Pyrin plays a role in remodeling the PSTPIP1 fibrils when it binds to them (Taskiran et al., 2012).

The main role of pyrin regulation of caspase 1 activation via converts caspase-1 into its active form through the interact with PSTPIP1 and ASC adaptor proteins and NF-κB activation. Caspase-1 is responsible conversion of pro IL-1β into IL-1β. This pathway involves other autoinflammatory disease related genes such as pyogenic arthritis, pyoderma gangrenosum and acne–PAPA syndrome (PSTPIP1), cryopyrinassociated period syndromes–CAPS (NLRP3) and deficiency of IL-1 receptor antagonist–DIRA (IL1RN). Understanding of these pathways can provide significant support for threapy of FMF disease (Chae et al., 2009; Soriano and Pras, 2014).

1.4 Role of Epigenetics in Gene Regulation

Epigenetics is the study of changes in gene function that can be mitotically and/or meiotically heritable which are not linked to changes of deoxyribonucleic acid (DNA) sequence (Horshuburg et al., 2015). The mechanisms underlying in epigenetic alterations (such as DNA methylation, histone modifications and RNA-associated silencing) can regulate gene expression and affect development of disease. In addition, many enviromental factors affect epigenetic mechanisms (Seo et al.,

2014). An epigenetic factor can act either directly or indirectly. There are two direct effects of epigenetics which are altering the availability of epigenetic enzymes and modifications of epigenetic pathways. Also, modification of signaling pathways is a indirect effect of the epigenetics (Kanherkar et al., 2014). Epigenetic regulation plays a major role in gene expression, DNA replication, recombination and repair, and is responsible for stem cell development and cellular differentiation. Furthermore, alterations in epigenetic modifications accompany the aging process and contribute to the pathogenesis of cancer and degenerative diseases (Hashimoto et al., 2010).

1.4.1 Chromatin structure

In eukaryotic organisms, DNA is packaged into chromatin within the nucleus (Yamaguchi et al., 2014). Chromatin consists of DNA, histones and other protein complexes that assist the dynamic changes occurring during nuclear process such as DNA replication, regulated-transcriptional and post-transcriptional events, DNA repair and recombination (Verdone et al., 2006).

Nucleosomes are the primary units of chromatin structure which consist of an octamer of two copies each of four core histones (H2A, H2B, H3, and H4) that ~147 bp of DNA are wrapped around it to form a nucleosome core (of relative molecular mass 206K) in 1.65 turns, left-handed superhelix (Luger et al., 1997; Rosenfeld et al., 2009). Structural organisation of nucleosome and chromatin packaging shown in Figure 1.3. Core histones are composed of the histone fold, the histone fold extension and the histone tails. The histone tails are between 16 to 44 amino acids in length; the N-terminal tails of histones are not associated with a secondary structure and are found to be estimated out of the nucleosome core and chromatin structure. Also, in some cases a carboxyl-terminal tail is also recognizable such as histone H2A (Luger et al., 1997). This highly conserved nucleoprotein complex occurs every 200 ± 40 bp throughout all eukaryotic genomes. Adjacent nucleosomes are linked by a segment of linker DNA to form a 30 nanometre (nm) fiber, and the addition of histone H1 to each nucleosome lends stability to and facilitates the formation of further higher-order structures (Jiang et al., 2004).

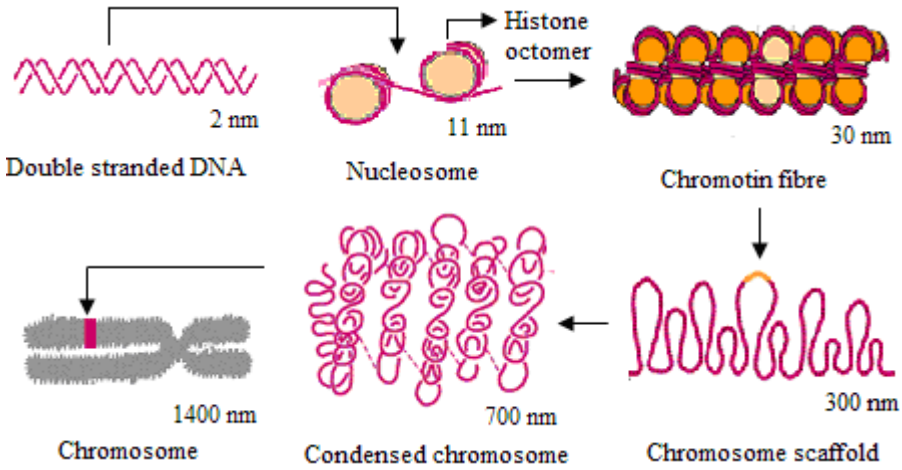

Figure 1.3: Structural organization of nucleosome and chromatin packaging, adopted from (Luger et al., 1997).

The chromatin complex include two major functional domain; either euchromatin or heterochromatin regions. Euchromatin is an open structure that consists of highly actively transcribed genes, while heterochromatin is a contracted and closed structure, which represents transcriptionally inactive conditions as a result of blocking DNA accessibility (Jiang et al., 2004). Heterochromatin regions has been classified into facultative and constitutive heterochromatin. Facultative type may form at various chrosomal regions which generally contains genes. But, constitutive type happen same genomic regions which usually do not contains genes (Saksouk et al., 2015). The heterochromatic regions are mostly found at centromere, pericentromeric regions and telomere (Karpen and Allshire, 1997). Identification of these two types of chromatin leds to the hypothesis that differences in chromatin structure might be associated with tissue-specific or temporal differences in gene expression (Jiang et al., 2004).

1.4.2 DNA methylation

The methylation of DNA at CpG dinucleotides is a key epigenetic modification in the human genome essential for regulatory and developmental processes (Huh et al., 2013). DNA methylation control gene expression by modulation of DNA–protein interactions, in many eukaryotes (Pomraning et al., 2009). DNA methylation mainly occurs at the carbon 5 (C5) position of about %70-80 of cytosine bases as described by Bird (2002) within CpG dinucleotides termed ‘CpG islands’ that typically contain around 5-10 CpGs per 100 bp which often located within gene promoters and regulatory regions. But, non-CpG methylation has been observed at relatively

low levels in pluripotent stem cells (Auclair and Weber, 2012; Guo et al., 2011). Methylated regions of DNA play an important role in transcriptional repression which are reformed in a closed configuration (heterochromatin) whereas unmethylated regions referred to active transcription which are packaged into open structure (euchromatin) formation (Horsburgh et al., 2015).

The primary focus of DNA methylation studies which is analysis of DNA methylation at TSSs showed that the methylated CpG islands depress transcriptional initiation and therefore, DNA methylation can be regarded as a silencing epigenetic mechanism at the promoters (Hashimshony et al., 2003; Kass et al., 1997; Venolia and Gartler, 1983). Methylation degrees in mammalian promoters suggests that methylation occurs at only a small percentage of CpG dinucleotides and inhibits transcription of only a small subset of genes in differentiated cells. Many of these repressed genes are germline-specific, including pluripotency genes, indicate that methylation is a critical mechanism by which to suppress key genes during differentiation (Handy et al., 2011).

Hypermethylation is hardly associated with heterochromatin and transcriptional silencing. DNA methylation disturbances patterns have been associated with dysregulation of gene expression in cancer cells, specially down-regulation of genes with tumor suppressor functions by hypermethylation of their promoter regions (Laurent et al., 2010). Our preivous study was shown that reduced gene expression (p=0,031) and increased methylation level of exon 2 in FMF patients compared to healthy control (p=0,049) (Kirectepe et al., 2011a).

In the addition of a methyl group on the C5 of the cytosine in CpG-rich regions (CpG islands), thereby creating 5-methylcytosine (5mC), and is catalyzed by enzymes of the DNA methyltransferase (DNMT) family, with methyl group donor generally being S-adenosyl methionine (SAM) (Figure 1.4) **(**Liyanage et al., 2010; Auclair and Weber, 2012). DNMTs can introduce methylation marks (*de novo* methylation) and maintain them after the genome is replicated (maintenance methylation), making DNA methylation a long-term and potentially heritable mark (Kohli and Zhang, 2013).

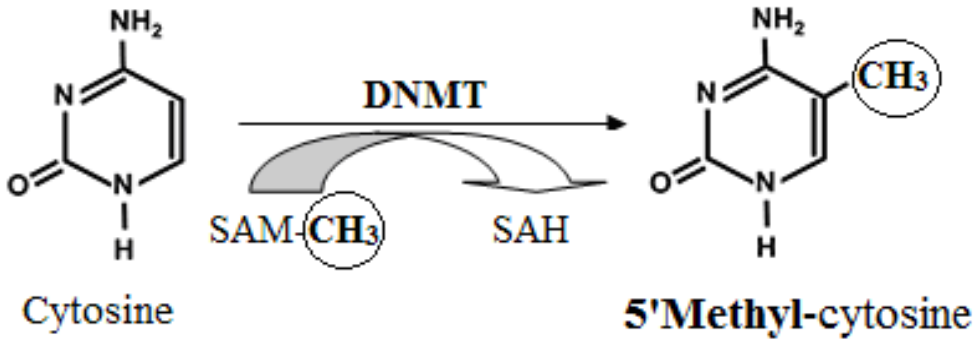

Figure 1.4: Schematic representation of DNA methylation, which converts cytosine to 5'methyl-cytosine via the actions of DNA methyltransferase (DNMT), adopted from (Horsburgh, 2015).

As a member of family, DNMT1 isoform, DNMT1 O is responsible for maintaining DNA methylation during DNA replication. Replication creates hemimethylated DNA sites, which are the preferential substrates for DNMT1 that copies patterns of CG methylation onto the newly synthesized DNA strand. During S-phase of DNA replication, DNMT1 localizes at sites of DNA via interactions with proliferating cell nuclear antigen (PCNA), and ubiquitin-like with PHD and ring finger domains 1 (UHRF1) (also known as NP95), a factor that binds hemimethylated CGs and is required to collect DNMT1 at sites of hemimethylation (Auclair and Weber, 2012).

DNMT3 family members, DNMT3A and DNMT3B, complexed with DNMT3L are responsible for *de novo* DNA methylation (Jia et al., 2007). DNMT3A and DNMT3B enzymes carry out *de novo* DNA methylation during development. Although both enzymes dominate distinct target specificities and expression patterns, they are greatly homologous. DNMT3B is more common in early embryonic stages and is the main enzyme responsible for the acquisition of DNA methylation during implantation. However, DNMT3A is expressed in later embryonic stages and differentiated cells. Morever, DNMT3A and DNMT3B join in the maintenance by methylated sites that were missed by DNMT1. DNMT3L lacks a functional methyltransferase domain and is proposed to play the role of co-factor, enabling the *de novo* methylation function of DNMT3A and DNMT3B and promotes their recruitment to chromatin (Auclair and Weber, 2012).

DNMT2 has a weak DNA methyltransferase activity (Hermann et al., 2003) and it is not essential for either global de novo or maintenance of the DNA methylation in embryonic stem cells (Okano et al., 1998).

1.4.3 Histone modifications

Histones are protected proteins that package and organize DNA. These proteins can be grouped in core histones (H2A, H2B, H3 and H4) and linker histones (H1 and H5). The linker histones bind to the DNA by sealing off the nucleosome at the location where DNA enters and leaves (Ronderos and Ortiz, 2011). Thanks to post-translational modification of the core histones, chromatin is either closed or open structure, thence regulating gene transcription and serving as a crucial epigenetic mechanism (Seo et al., 2014). Histones are modified at over 60 different sites, which give rise to huge number of modifications on histones. Especially the amino-terminal (N-terminal) ends of the amino acid residues of histones are subject to innumerable post-translational modifications including acetylation, methylation, ubiquitylation and sumoylation of lysine (Lys or K) residues, methylation of arginine (Arg or R) residues, phosphorylation of serine (Ser or S) and threonine residues (Thr or T) (Hashimoto et al., 2010; Kouzarides, 2007). Different classes of modifications have been identified on histone as shown Table 1.1 (Kouzarides, 2007). Histone modifications affect the histone-histone and histone-DNA interactions, in this way affecting the nucleosome structure and how it interacts with the DNA. The reversible post-translational modifications of histones can regulate the chromosome structure and gene expression (Kouzarides, 2007; Wilson, 2008; Hodges, 2009; Orphanides and Reinberg, 2000). The relation of the histone marks to a specific transcriptional state is mediated by histone-binding proteins that recognize the histone modifications and determine the downstream consequences (Warrier, 2010). These biochemical modification of histone tails referrred to “histone code” (Espeda et al., 2004). The enzymatic mechanism responsible for maintaining the chromatin dynamics by either modifying the histone tails or removing them also contribute to the confusion of the histone code. The main actors in the histone code are writers, readers or erasers designed by chromatin domain which are transmit adjecent or opposite signals within their netwok, referred to as ‘cross talk’. A enzyme that writer is responsible to introduces a post-transcriptional modification into a protein such as histone methyltransferases (HMTs) whereas eraser has a opposite role such as histone demethylases (HDMs). Also, reader is a protein that binds specifically to a post-transcriptionally modified protein such as PHD-containing effector (Warrier, 2010).

Table 1.1: Histone modifications and their functions, adopted from (Kouzarides, 2007).

Chromatin Modifications	Residues Modified	Functions Regulated
Acetylation	**K**-ac	Transcription, Repair, Replication, Condensation
Methylation (Lysines)	**K**-me1 **K**-me2 **K**-me3	Transcription, Repair
Methylation (Arginines)	**R**-me2 **R**-me2a **R**-me2s	Transcription
Phosphorylation	**S**-ph **T**-ph	Transcription, Repair, Condensation
Ubiquitylation	**K**-ub	Transcription, Repair
Sumoylation	**K**-su	Transcription
ADP ribosylation	**E**-ar	Transcription
Deimination	**R > Cit**	Transcription
Proline isomerization	**P-cis > P-trans**	Transcription

Normally, histone proteins are positively charged and strictly associate with DNA that is negatively charged, which leads to chromatin compaction and blocked gene expression. However, if the positive charges of the histone proteins are changed by the addition of an acetyl group (i.e., histone acetylation), the DNA and histones form a more relaxed (open) and favors gene expression. Specific enzymes known as histone acetyltransferases (HAT) and histone deacetylases (HDACs) are resposible to addition and removal of these acetyl groups, respectively. Other post-translational histone modifications include methylation and phosphorylation; depending on its location, histone methylation may be a marker of active or inactive regions of chromatin (Wilson, 2008).

Most modifications are distributed in different localized patterns within the upstream region, the core promoter, the 50 end of the open reading frame (ORF) and the 30 end of the ORF. Actually, the location of a modification is firmly regulated and is critical for its effect on transcription (Li et al., 2007).

1.4.3.1 Histone lysine methylation

Adding a methyl group via covalent bond from SAM substrates to the nitrogen atoms on the side chains of lysine and arginine residues result in histone methylation. Although, lysine residues can be methylated mono- (me1), di- (me2) or tri- (me3) forms, ariginine residues can only be methylated mono-(me1) or di-(me2) forms (Kouzarides, 2007).

Histone lysine methylations can be associated with transcriptional activation, such as H3K4, H3K36 and H3K79 methylations, and repression, such as H3K9, H3K27 and H4K20 methylations, in a context-dependent manner, commonly referred to as euchromatin and heterochromatin modifications, respectively (Di Lorenzo and

Bedford, 2011; Li et al., 2007). Similarly, arginine monomethylation can be associated with both transcriptional activation and repression, yet symmetric arginine dimethylation is connected repression and asymmetric arginine dimethylation is associated with activation (Di Lorenzo and Bedford, 2011).

Generally, H3 lysine acetylation, associated with gene activation, and histone H3 lysine methylation (H3K9me), associated with either gene activation or repression depending on the site of methylation. As an added layer of regulation, lysine residues can be mono- (me1), di- (me2), or tri (me3) methylated by HMTs. Trimethylation of H3K9 (H3K9me3), which is usually related to heterochromatin regions and therefore, gene repression. This modification is catalyzed by the conserved mammalian ortholog of the *Drosophila* suppressor of position-effect variegation, Su(var)3–9-related HMTs, SUV39H1 in humans, and Suv39h1 in mice. H3K9me3 plays roles in gene silencing by recruiting repressors and cofactors including histone deacetylases (HDACs) and heterochromatin protein-1. Histone Kme is a more dynamic process. HDMs such as lysine-specific demethylase 1 (LSD1) and the jumonji domain 2 (JMJD2) family members able of reversing histone H3K4 and H3K9 methylation, respectively (Villeneuve et al., 2008). Recent studies demonstrated that H3K9me3 can also be associated with transcriptionally active gene regions. However, no significant H3K4me3, which is coupled to transcription-associated H3K9me3 (Zeng et al., 2009).

The early studies of histone methylation distributions shown that there is H3K4me3 marks at the promoter regions and transcription start sites (TSSs) of transcribed genes (Barski et al., 2007). Furthermore, H3K4me2 marks were mainly identified within the active gene bodies and H3K4me1 marks were detected on active enhancers and active gene bodies (Barski et al., 2007; Heintzman et al., 2009). But, analysis of H3K4me3 distribution at the genome-wide level indicated that this mark is associated with CpG-rich promoters regardless of their transcriptional activity (Guenther et al., 2007; Mikkelsen et al., 2007). On the other hand, H3K4me2/me3 sites were found to be contrarily correlated with DNA methylation at the promoters (Meissner et al., 2008; Ooi et al., 2007). H3K4me3 mark catalyzed by Trithorax protein complexes, is associated with active transcription. Mixed-lineage leukemia-1 methyltransferase, a mammalian homolog to Trithorax, confirms colocalization with H3K4me3 (Pan, 2007).

Furthermore, chromatin modifications play a vital role in pre-mRNA splicing. It was shown that H3K4me3 histone modification facilitate the production of pre-mRNA maturation (Sims et al., 2007). Altough, histone marks associated with transcription initiation and transcription repression, such as H3K4me3 and H3K9me3, respectively, were also shown to be associated with splicing gene-specifically (Podlaha et al., 2004).

1.4.4 Relation of DNA methylation and histone modifications

Two epigenetic regulatory platforms, DNA cytosine methylation together with histone modifications, necessary for multiple developmental and disease processes (Li et al., 2011). The different modifications do not act independently of each other (Brinkman et al., 2012). Enzyme mediated chemical modifications of DNA is often associated with gene repression. While CpG methylation is essential in development, inappropriate CpG methylation in tumor suppressor genes is associated with cancer (Choy, 2010). Histone post-translational modifications (PTMs) that are themselves regulated by lysine acetyltransferases (KATs) and HDACs, play a role by blocking or promoting DNA methylation via specific histone acetylation or methylation marks (Liyanage et al., 2010).

Chromatin structure maintains through dynamics of DNA methylation and histone PTMs, either open or closed chromatin structures are obtained to assist transcriptional activation or repression, respectively (Liyanage et al., 2010).

DNA methylation and deacetylation of histones connection has more recently been elucidated, where the methyl CpG binding protein 2 (MeCP2) directly recruit HDAC activity to silence gene expression. Methylation of the DNA induce a deacetylation of histones and thus promote heterochromatisation. These results suggest that two gene regulation mechanisms, DNA methylation and histone deacetylation, can be linked by MeCP2. Therefore, DNA methylation and histone deacetylation functions are common mechanistic pathways to repress transcription (Fuks et al., 2003; Jones et al., 1998; Nan et al., 1998). The histone H3 tail is necessaary for DNA methylation by supplying a direct contact with DNMT3A-DNMT3L. However, transformation of a chromatin modification status into DNA methylation mechanism is left unexplored (Li et al., 2011).

In mammals, the binding of UHRF1 (also known as Np95 or ICBP90) to methylated H3K9 chromatin provides for the maintenance of DNA methylation through regulation of the stability of DNMT-1 (Garwin Pichler et al., 2011; Rothbart et al., 2011). Functional connections between 5 hydroxymethyl cytosine (5hmC) and histone lysine methylation identified, by the discovery that UHRF1 and MeCP2 can also bind to 5hmC. Non-methylated DNA in CpG islands can act as part of a genomic signature to recruit H3K4 and H3K27 trimethylations, and to exclude H3K36 methylation. But, understanding how de novo DNA methylation is targeted during development remains poorly understood (Rose and Klose, 2013).

1.5 Chromatin Immunoprecipitation (ChIP) Assay

Chromatin immunoprecipitation (ChIP) is a strong method of enriching for the DNA sequences which are related to proteins in genomes. This method is powerful to identify *in vivo* protein-DNA interactions which are very important for most of cellular processes such as DNA replication and repair, chromosomal stability, cell cycle succession, and epigenetic regulation through silencing and activating mechanisms. ChIP has been commonly used to study histones, transcription factors, and other protein binding sites (O'Neill and Turner, 1996; Orlando et al., 1997; Solomon and Varshavsky, 1985).

The first ChIP protocol was developed by Gilmour and Lis (1984, 1985, 1986) to monitor RNA polymerase II (RNA Pol II)/ DNA association in *Escherichia coli* and *Drosophila melanogaster* using ultraviolet (UV) light to cross-link proteins covalently to DNA (Gilmour and Lis, 1984). The use of formaldehyde for fixation of protein in ChIP was generated by Solomon et al. (1988). Then, formaldehyde was commonly used in ChIP experiments for most organisms. The aim of a genome-wide ChIP experiment are to map the binding sites of a target protein with maximal signal-to-noise ratio and exactness across the genome (Pamela et al., 2011). ChIP assay consists of six main steps which are crosslinking the protein to the DNA, isolation of chromatin from a nuclear extract, sonication or enzymatic digestion to fragmentation of chromatin to target size of 300-600 bp, immunoprecipitation with an antibody specific for the factor, reverse-crosslink, purify of enriched DNA and identification of associated DNA sequences (Yamaguchi et al., 2014; Pamela et al., 2011). In order to analysis of protein associated DNA fragments, ChIP method can be coupled to

various downstream applications including polymerase chain reaction (PCR) and qPCR, southern blot analysis described by Orlando et al (1997), western blot analysis described by Wells and Farnham (2002), microarray hybridization (ChIP-chip,) and ChIP sequencing (ChIP-Seq) (Landt et al., 2012).

ChIP can be classified into two main categories; crosslinked ChIP (X-ChIP) (Orlando et al., 1997) or native ChIP (N-ChIP) (O'Neill and Turner, 2003). In X-ChIP, DNA- protein complexes are usually reversibly crosslinked, either chemically or with UV light and chromatin is then fragmented by sonication to an approximate size range of 200-1000 bp, with an average length of 500 bp. Usual X-ChIP protocol summarized in Figure 1.5. N-ChIP uses unfixed chromatin fragmented mainly by nuclease digestion. For both types of ChIP, the sheared chromatin is then incubated with specific antibodies and antibody-protein-DNA complexes are precipitated by agarose or paramagnetic beads coated with protein A/G followed by a series of washes. After reverse-crosslink and digestion of proteins, the enriched DNA fragments are purified (Koorosh, 2012).

The main limitaion of ChIP its inherent variability. ChIP is a multi-step procedure and hence some level of variability is to be expected. The variability in the final results may arise from variability in the crosslinking step, immunoprecipitation or the protein-DNA washing stage. A number of carefully chosen controls are needed to account for the variability in these steps. Other limitations of ChIP analysis dependence on the availability of a specific antibody as well as broad expression of the DNA-binding protein of interest (Mukhopadhyay et al., 2008).

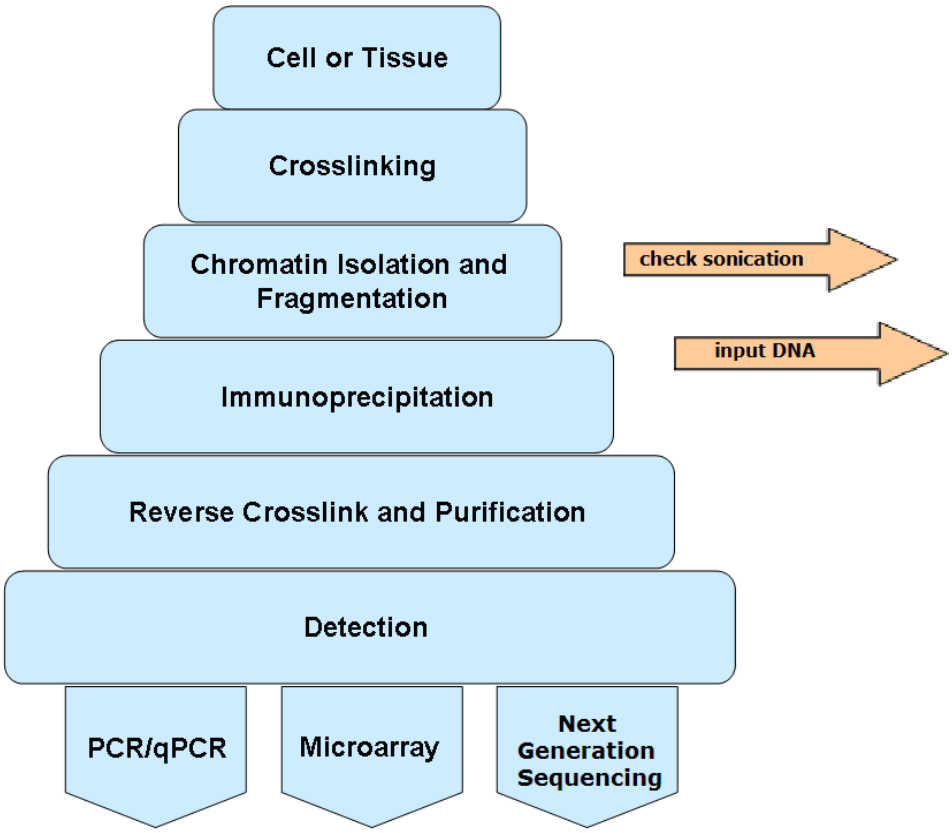

Figure 1.5: ChIP procedure, adopted from (Landt et al., 2012).

1.6 Chromatin Immunoprecipitation Sequencing (ChIP-Seq)

DNA fragments obtained from ChIP can identified by deep sequencing (ChIP-Seq) using the next generation sequencing (NGS) platforms (Park, 2009). ChIP-Seq has now been commonly used for many transcription factors, histone modifications, chromatin modifying complexes, and other chromatin-associated proteins in a vast variety of organisms (Landt et al., 2012). ChIP-Seq enables identification of genome regions occupied by chromatin associated proteins and defining functionally important regulatory elements. ChIP-Seq experiment yield several million short nucleotide sequences corresponding to the possible binding sites of a given protein. These sequences, called reads, are then mapped to a reference genome, supplying a list of genomic interaction sites. Most of these reads uniquely map to the + (sense) or − (antisense) strand of the corresponding genome sequence. The positions data set may then be searched for reads distribution around specific locations or at cis-regulatory elements (Schmid and Bucher, 2007; Chojnowski et al., 2014). In a ChIP reaction, the majority (~60-99%) of DNA fragments (and therefore of sequence reads) are background, while the minority corresponds to DNA fragments to which

the transcription factor or histone mark of interest was crosslinked at the beginning of the experiment (Pepke et al., 2009).

Different protein classes have distinct modes of interaction with the genome (Pepke et al., 2009):

1. Point-source factors and certain chromatin modifications that includes most sequence-specific transcription factors, their cofactors and transcription start site or enhancer-associated histone marks are localized at specific positions. These positions generate highly localized ChIP-Seq signals (Landt et al., 2012).

2. Broad-source factors are associated with large genomic domains. For examples, certain chromatin marks (H3K9me3, H3K36me3) and chromatin proteins associated with transcriptional elongation or repression (e.g., ZNF217) (Krig et al., 2007).

3. Mixed-source factors can show both point and broader patterns of binding, depending of the target gene. RNA polymerase II as well as some chromatin modifying proteins (e.g., SUZ12) act in this way (Squazzo et al., 2006).

ChIP-Seq advantages are base pair resolution, less expensive for whole genome analysis, greater genome coverage as the only limitation is the alignability of sequenced tags, the absence of noise generated as a result of cross-hybridisations or labelling artefacts, larger dynamic range as the enrichment levels are independent of signal intensities which are affected by saturation points, requirement for significantly lower amounts of starting material (~10 ng), less amplification for genome-wide analysis which can even be completely avoided in the case of single-molecule sequencing (Park, 2009). Workflow of the central step in the ChIP-Seq procedure shown in Figure 1.6 (Liu et al., 2010).

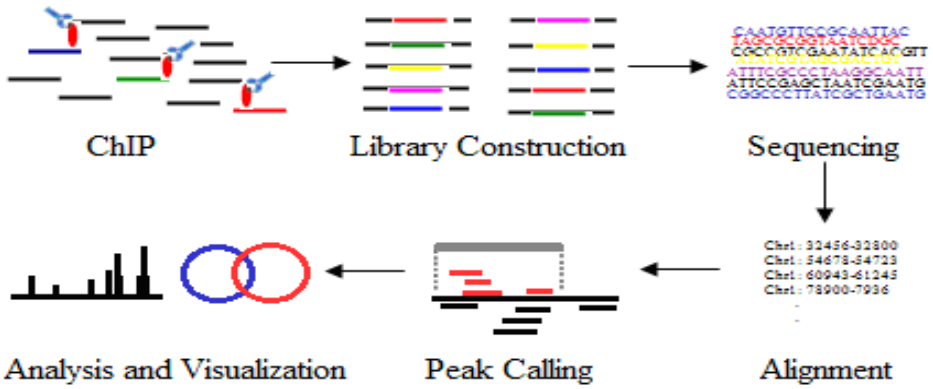

Figure 1.6: Flow scheme of the central step in chromatin immunoprecipitation sequencing, adopted from (Liu et al., 2010).

The ChIP-Seq library is consist of the immunoprecipitated short DNA fragments that carry two adapter sequences at both ends. The PCR-amplified library is subjected to size selection in the ~200-300 bp range. In single-end (SE) sequencing, ChIP DNA sequencing performed from the 5′-end. But, in paired-end sequencing, it is possible to perform sequencing from both ends. The advantageous of its in mapping the repetitive elements and long-range chromatin interactions (Fullwood and Ruan, 2009). Illumina Genome Analyzer is the most widely used NGS platform for the ChIP-Seq studies, although other platforms such as Applied Biosystems' SOLiD and the Helicos platform available now (Park, 2009).

1.7 Bioinformatic Analysis

Analysis of ChIP-Seq data generally include quality controls, alignment to a reference genome, peak calling, genomic annotation, generation of raw signal tracks for visualization (Barozzi et al., 2011).

High throughput sequencing usually generate up to hundreds of millions of 25 to 75 bp sequences (short reads) from the 5′ ends of enriched DNA fragments (Feng et al., 2012). Effective analysis of ChIP-Seq data requires sufficient coverage by sequence reads (sequencing depth). Sequence depth depends on genome size and the number and size of the binding sites of the protein. For mammalian ChIP-Seq narrow factor 20 million reads may be adequate and broader factor require more reads, up to 60 million. After ensure that the sequence depth short reads should be filtered by applying quality cut-off (Bailey et al., 2013).

The remaining reads can be mapped using mappers such as Bowtie, BWA, SOAP or MAQ to a reference genome. While many mapped reads are spreaded throughout the genome, others are found in clusters constituting read-enriched regions, which represent the locations of transcription factor binding or histone marks. For the majority of transcription factors and several histone modifications such as H3K4me3, ChIP-Seq reads are often concentrated in narrow peaks of a few hundred base pairs. However, for some transcription factors such as RNA Pol II and other histone modifications such as H3K36me3, read enrichment regions can be broad, spanning up to tens of thousands of base pairs. Factors such as GC content, read mappability, DNA repeats, copy number variations and local chromatin structure can influence read distribution at different locations of the genome. Therefore, sequencing control

samples of sonicated chromatin is recommended as an additional measure to better eliminate background biases so as to reliably identify read-enriched regions obtained from ChIP-Seq. The percentage uniquely mapped reads reported by mapper data, above 70% is normal, whereas less than 50% may be cause for concern (Feng et al., 2012; Bailey et al., 2013).

Then, applying filter of sequenced reads are aligned to the genome based on duplicate level, mapping quality score, genomic uniqueness, insertion size and orientation (for paired end reads only) and estimation of library complexity. After generating uniquely aligned DNA fragments, the next step is identification of regions that are enriched in the sample relative to the control with statistical significance by the 'peak calling' algorithms (Park, 2009). Many number of peak caller avaliable and may be selected based on binding profile such as sharp, broad, and mixed. Often, MACS can be used for sharp binding sites, which are found for protein-DNA binding or histone modifications at regulatory elements. However, SICER can be used for broad binding domains, which are linked to histone modifications marking domains, for example, transcribed or repressed regions (Park, 2009; Barozzi et al., 2011).

MACS has been demonstrated the best performance and able to model the shift size of the tags using the strand information from the most enriched genomic regions, defined through the mfold parameter (Barozzi et al., 2011). The major function of SICER algorithm is to pool together signals from nearby nucleosomes that are in the same modification state and able to systematic evaluation of statistical significance of identified ChIP-enriched regions against control library. Actually in SICER, reads on ChIP-enriched regions can be identified and used for profiling and other quantitative analysis (Xu et al., 2014).

An ideal peak calling algorithm should considered the strand-specific pattern at any binding location, correct for the local variation shown by input DNA, adjust for sequence alignability, and measure the expected ratio of incorrectly discovered sites to those that are found to be significant by the false discovery rate (FDR). The FDR suggests a sensible measure of the balance between the number of true and false positives that is automatically calibrated and easily interpreted. The q value, an extension of the FDR, associated with each tested feature and similar to the p value, except it is a measure of significance in terms of the false discovery rate rather than

the false positive rate. The correctness of peak caller can be validated by large set of sites via qPCR (Park, 2009; Storey and Tibshirani, 2003).

The most common downstream analyses include discovery of binding sequence motifs by motif finding algortihm programs such as MEME, MDScan, Weeder. Another is annotation of peaks on the genome associate with genomic features, such as the TSS, exon/intron boundaries and 3′end of genes and, visualization of peaks using such programs (for example, Genome Browser, IGV and IGB). Gene Ontology (GO) analysis can be applyed to see whether a particular molecular function or biological process is over-represented in those genes. Advanced analysis consists of discovery of novel elements based on ChIP-Seq data. Following with SNP analysis ChIP-Seq data can also be used to investigate allele-specific binding and modification (Park, 2009).

Table 1.2: Bionformatic tools used for ChIP-Seq data.

	Tool name	Used for	Reference
QC and manipulation	**FastQC**	Read quality reports	Johnson, J.
	Filter FASTQ	Filter reads by quality and length	Blankenberg, D., et al.
Mapping	**Bowtie2**	Map reads against reference genome	Langmead, B.
SAM Tool	**Rmdup**	Remove PCR duplicates	Li, H., et al.
	Slice BAM	Visualization of mapped reads	Li, H., et. al.
Peak Calling	**MACS**	Identification of reads on the ChIP-enriched regions	Zhang, Y., et al.
	SICER	Identification of reads on the ChIP-enriched regions	Zanc, C., et al.
Annotation and Visualization	**PAVIS**	Identification of relevant genomic context for peaks	Huang, W., et al.
	Nebula	Annotation of genes with ChIP-Seq peaks	Nebula http://nebula.curie.fr/
	IGV	Visualization of ChIP-Seq peaks	Integrative Genomics Viewer https://www.broadinstitute.org/igv/
	UCSC	Visualization of ChIP-Seq peaks	UCSC Genome Browser https://genome-euro.ucsc.edu
Gene Ontology	**DAVID**	Identify enriched biological themes	Huang, D. W., et al.
Operate on Genomic Intervals	**Intersect**	Detect overlapping intervals of two datasets	Usegalaxy https://usegalaxy.org/
	Subtract	Detect non-overlapping intervals of two datasets	Usegalaxy https://usegalaxy.org/

1.8 The Aim of the Study

Presence of Familial Mediterranean Fever (FMF) patients without MEFV mutations (Ben-Zvi et al., 2015) and increased MEFV second exon methylation in FMF patients compared to controls (Kirectepe et al., 2011a), have urged us to explore more of the chromatin dynamics of the FMF patients. To this end first we wanted to analyse histone modifications in FMF patients during inflammatory attack and attack-free times and compared with healthy controls. Chromatin immunoprecipitation (ChIP) is carried out in peripheral blood moconuclear cells (PBMCs) (approximately 1 million) isolated from 10 FMF patients (during attack and attack-free period) and same number age matched healthy volunteers. In order to detect the modifications binding sides on DNA, antibodies against two different histone modifications, H3K9me3 (heterochromatin mark) and H3K4me3 (euchromatin mark), with normal IgG as a negative control and RNA Pol II as a positive control from rabbit in ChIP are used. The ChIP experiment coupled with next generation sequencing (ChIP-Seq) will done in order to find out the genome regions enriched with euchromatin and heterochromatin marks. Candidate genome regions are detected via bioinformatic analysis of the ChIP-Seq data and any significant change in histone composition is validated by standard PCR.

2. MATERIALS AND METHOD

2.1 Materials and Laboratory Equipment

2.1.1 Used equipments

The laboratory equipment used in this study is listed in Appendix A.

2.1.2 Used chemicals, enzymes, markers, commercial kits and buffers

The chemicals, enzymes, markers and commercial kits used are given in Appendix B with their suppliers. The compositions and preparation of buffers are given in Appendix C.

2.2 Collection of Samples

Study groups include 10 patients with FMF (6 male/4 female) during attack and attack-free periods were collected from Cerrahpaşa Faculty of Medicine, Department of Rheumatology, and 10 age and sex matched healthy volunteers (5 male/5 female). Peripheral blood samples were collected from each individual into 10 or 20-milliliter (mL) EDTA tubes were kept room temperature up to 6 hours until the next step.

2.3 Peripheral Blood Mononuclear Cell (PBMC) Isolation from Whole Blood

PBMCs were separated by density gradient centrifugation method using Histopaque–1077 (Sigma-Aldrich) solution. All solutions and blood samples were warmed to 15-25^{o}C. Using a sterile pipet, fresh heparinized blood (10 mL or 20 mL) combine with equal volume of room temperature phosphate buffered saline (PBS) in a sterile 15 or 50 mL centrifuge tube according to volume of blood and mixed well. Histopaque put a bottom of the 15 mL or 50 mL centrifuge tube and an equal volume diluted blood slowly layered over the solution in 2:1 ratio at a 45°C angle. After the centrifuge 30 minutes (min) at 400 x *g*, 22°C with no brake, PBMCs layer that are located on top of to histopaque solution harvested to new a sterile 50 mL centrifuge tube using a sterile pipet and washed twice with 10 mL PBS 10 min at 1000 rpm,

22°C. The PBMCs were resuspended in 10 mL RPMI and total number of PBMCs detected. These samples stored -80°C until assayed.

2.3.1 Cell counting and determining the viability

PBMCs were counted using a hemocytometer chamber and cell viability was determined by trypan blue dye exclusion. 8 µL was taken from suspension and cells were exposed to Trypan blue dye (2 µL). 10 µL of cells from trypan blue-medium mixture was filled on Dual-chamber FisherLab hemacytometer and cells were counted under a light microscope, non-viable cells were observed as stained while viable cells excluded the stain.

The cell number calculation is as follows:

10^4 (constant number) x Amount of counted cell = Cell number/mL

Total cell number = Cell number/ mL x Total volume of cells

2.4 Chromatin Immunoprecipitation (ChIP)

2.4.1 Crosslink of chromatin

Formaldehyde was used as a chemical reagent in order to fixation of proteins. Approximately 1 x 10^6 cells were used per immunoprecipitation (IP). Formaldehyde solution (34,5%) was added to a final concentration of 1M and the sample was inverted 3 times to mix and incubated at room temperature for 10 min. Then 1 M glycine was added to a final concentration of 125 mM to quench unreacted formaldehyde and stop over-crosslinking. The sample was inverted to mix and incubated at room temperature for 5 min. The sample was kept on ice from this point on. After centrifugation at 1000 rpm for 5 min at 4˚C, the supernatant was removed and the pellet was resuspended in 10 mL of chilled PBS. This wash was then repeated once.

2.4.2. Optimization of sonication

2.4.2.1 Cell lysis buffer (CLB-SDS) optimization

Cell suspension exposed to cell lysis buffer (consist of 1% and 0,25% sodium dedocyl sulfate (SDS)) and DNA purified using ‘Zymo DNA Clean and Condensator Kit’ (section 2.4.9). Concentration and purity of DNA samples were measured by

Nanodrop (Thermo Scientific) at 260/280 nm, and optimum SDS concentration in cell lysis buffer was determined.

2.4.2.2 Preparation for sonication

The crosslinked cell pellet resuspended in 100 µL Cell Lysis Buffer (CLB, 1% SDS) containing 50X Protease inhibitor Cocktail II and incubated on ice for 30 min. The resuspend cell stored at -80˚C until the next step.

2.4.2.3 Optimization of the sonication conditions

Different power settings of the sonicators in addition to different duration and number of pulses were tested for optimase sonication conditions in HL-60 cell suspension. 1% of the samples were removed prior to the sonication for analysis of the unsheared DNA and 5% were removed after each sonication conditions in order to check of shared DNA length (200-1000 bp) on 1% agarose gel via UV light. Optimisation of sonication is as follows:

- Cell suspensions include $2{,}5x10^5$, $5x10^5$ and $1x10^6$ cell in 125 µL, 250 µL and 500 µL cell lysis buffer in 1,5 mL eppendorf tubes, respectively, sonicated for 6 cycles (10 sec on/ 10 sec off, 10 sec on/ 50 sec off and 30 sec on/ 30 sec off) with 50 Watt (W) on ice.

- Cell suspnesion include $2x10^6$ cell in 500 µL cell lysis buffer in 1,5 mL eppendorf tube exposed to 1 cycle (10 sec on/10 sec off) sonication with 50 W on ice.

- $5x10^5$ cell suspension in 125 µL cell lysis buffer in 1,5 mL eppendorf tube sonicated for 10 cycles (10 sec on/ 10 sec off) with 50 W on ice.

- $1x10^6$ cell suspension in 250 µL and 500 µL cell lysis buffer in 1,5 mL eppendorf tube sonicated for 2 cycles (10 sec on/ 10 sec off), 3 cycles (10 sec on/ 10 sec off), 2 cycles (10 sec on/ 15 sec off) with 50 W on ice.

- $1x10^6$ cell suspension in 250 µL cell lysis buffer in 1,5 mL eppendorf tube sonicated for 1 cycle (30 sec on/ 30 sec off) and 12 cycles (10sec on/ 15sec off) with 50W on ice.

- $4x10^5$cell suspension in 200 µL and 400 µL cell lysis buffer in 1,5 mL eppendorf tube sonicated for 5 cycles (30 sesc on/ 30 sec off) with 50 W on ice.

- $12x10^6$ cell suspension in 300 µL cell lysis buffer in 1,5 mL eppendorf tube sonicated for 4 cycles (30 sec on/ 30 sec off) with 50 W on ice.

- $1,5x10^6$ cell suspension in 300 µL cell lysis buffer in 1,5 mL eppendorf tube sonicated for 5 cycles (30 sec on/ 30 sec off) with 50% amplitude on ice.

- $1x10^7$ cell suspension in 2mL cell lysis buffer in 15 mL falcon tube exposed to 4 cycles (30 sec on/ 30 sec off) with 50 W, 3cycles (30 sec on/ 60 sec off) and 10 cycles (30 sec on/ 30 sec off) with 30 W on ice.

- $1x10^7$ cell suspension in 2 mL cell lysis buffer in 15 mL falcon tube sonicated for 10 cycles (30 sec on/ 60 sec off) and 20 cycles (30 sec on/ 30 sec off) with 30 W on ice.

Sonicated sample was transferred to a 1,5 mL eppendorf tube and centrifuged at 13000 x *g* for 10 min at 4˚C. 50 µL of the supernatant was removed to analyse the sonication efficiency.

2.4.3 Agarose gel electrophoresis

For the observation of the fragmented DNA which is 200-500 bp length, 1% agarose gel is sufficient after reverse-crosslink and purification of DNA as a decribed in section 2.4.8 and section 2.4.9. The agarose gel contains 1,5 g agarose dissolved in 150 mL of 1X TAE buffer as well as 0,5 µg/mL ethidium bromide. To evaluate the length of the fragmented DNA, 50 or 100 bp marker was loaded into the first wells of the gel. 15 µL of the product were mixed with 3 µL of 6X loading dye to faciliate the precipitation and the observation of relative position with naked eye under UV light. The gel were run for an average of 40-60 min in 100 Volt (V) into 1X Tris-acetate-EDTA (TAE) buffer. Bands were monitored under UV light.

2.4.4 Sonication to shear genomic DNA

The sample in CLB (1% SDS) was transferred to a 1,5 mL eppendorf tube (up to 300 µL volume) or 15 mL falcon tube (up to 2 mL volume) according to volume. All samples were sonicated for 20 to 55 cycles (30 sec on/30 sec off) with 30 W on ice using Bandelin Sonoplus Sonicator. The ice was changed every 20 cycles to avoid heating of the sample. After sonication step, the sample was transferred to a 1,5 mL eppendorf tube and centrifuged at 13000 x *g* for 10 min at 4˚C. 50 µL of the supernatant was removed to analyse the sonication efficiency by performing DNA

purification kit (section 2.4.9) and gel electrophoresis (section 2.4.3). The rest of the supernatant was aliquoted and stored – 80˚C until the next step.

2.4.5 Optimization of immunoprecipitation

2.4.5.1 Checking of antibody and magnetic bead interaction

Western Blot method was used analysis of antibody and magnetic bead binding efficiency with anti human RNA Pol II antibody to understand whether bound and unbound to magnetic beads. 50 µL Protein A and Protein G magnetic beads was washed with PBS-Tween 20 (PBS-T) solution (0,02% Tween-20) for 3 times. 5 µg of antibody was added and incubated at +4 ºC for 2 hours (hr) on rotator. Then antibody eluted with 50 mM fresh Glycine solution (pH:2,8) and incubated 15 min at room temperature. To obtain supernatant, beads were removed via magnetic separator and this step was repeated.

Bradford assay

For bradfords assay, total protein was used which generated form HL-60 cells and PBMCS. Standards with known concentrations and samples were brought to room temperature (18-25ºC) and 5 µL of standards and samples were added into wells of a 96-well microplate. All standards and samples were added in duplicate in order to avoid misleading. Then, 1 volume of Bradford dye was added to 4 volumes of distilled water to prepare the dye. 195 µL of diluted Bradford dye was added into each well. Finally, Optical Density values were read at 595 nm, using a microplate reader.

SDS-polyacrylamide gel electrophoresis of proteins (SDS-PAGE)

SDS polyacrylamide gel electrophoresis is a technique widely used to separate proteins according to electrophoretic mobility. The proteins are separated in gel according to their size. In this study, 5% stacking gel and 12% separating gel were used. Samples were brought to room temperature (18-25ºC). 20 µg of each sample was mixed with 5 µL of 4x loading dye, and mixtures were vortexed gently. Samples were boiled 95ºC for 5 min to gain primary structure, and transferred onto ice immediately to prevent protein renaturation.

Western blotting

Western blot method is used to check magnetics beads and antibody interaction. 25 µL of sample and 5 µL of marker were loaded into 5%-12% SDS-PAGE gels. Protein separation was done by electrophoresis for 2 hr at 120 V. Proteins were transferred onto nitrocellulose membranes from the gels by a semi-wet electro-blotting system. Transfer was done at 20 V overnight. Membranes were incubated with blocking solution (5% non fat dry milk) for 2 hr at room temperature. Primary antibodies (RNA pol II) were diluted in 5% non fat dry milk. Membranes were incubated with primary antibody solutions overnight at 4^{o}C. Membranes were washed with PBS-T for 5 min at room temperature twice. Membranes having were incubated with secondary antibody solutions for 2 hr at room temperature. Membranes were washed with PBS-T for 5 minutes at room temperature for 4 times. Membranes were incubated with BioRad Amplification Reagent Solution (from BioRad Western Blot Amplification Module) for 10 min at room temperature. Membranes were washed with 20% dimethyl sulfoxide (DMSO) solution for 5 min at room temperature. DMSO washing step was repeated three more times for a total of four washes. Membranes were washed with PBS-T for 5 min at room temperature twice. Membranes were incubated with 1:1000 diluted Streptavidin-HRP (from BioRad Western Blot kit) for 30 min at room temperature. Streptavidin-HRP was diluted in 5% non fat dry milk. Falcon tubes were covered with aluminium folio to avoid light. Membranes were washed with PBST for 5 min at room temperature twice. 18 mL distilled water, 2 mL Opti-4CN diluent, and 400 µL Opti-4CN substrate (from BioRad Western Blot kit) were mixed and transferred into tubes. Tubes were covered with aluminium folio and incubated for 15 min at room temperature. Membranes were washed with distilled water when the bands became visible. The membrane was exposed to X-ray film for a certain time and then developed in Kodak Medical X-ray Processor according to manufacturer's instruction.

2.4.6 Immunoprecipitation (IP) of crosslinked protein/DNA

For each immunoprecipitation reaction 50 µL Protein A and Protein G magnetic beads mix were washed 2 times with PBS-T (PBS, 0,02% Tween 20). An appropriate amount of antibody (described in section 2.4.10) and 50 µL of protein A and protein G magnetic beads combined and incubated 2 hr at 4˚C on a rotating wheel. Magnetic

beads were washed with 500 µL PBS-T ve CLB (no SDS) containing Protease Inhibitor Cocktail II (PIC II) and resuspended 50 µL CLB containig PIC II. 100 µL of sonicated material was diluted with 900 µL of ChIP dilution buffer containing 20 µL of PIC II for each immunoprecipitation reaction. 10 µL was removed from one of the IPs for input control, which represents the total amount of chromatin in the sonicated samples before IP. Fully re-suspended protein A and protein G magnetic beads added to diluted cell lysate. The IPs were incubated overnight at 4˚C on a rotating wheel. Protein A and Protein G magnetic beads were pelleted using a magnetic separator and the supernatant was discarded. The beads were then washed consecutively with 1000 µL of low salt immune complex wash buffer, high salt immune complex wash buffer and Tris-EDTA (TE) buffer for 2 times. The samples were incubated for 5 min at 4˚C on a rotating wheel for each wash.

2.4.7 Elution of protein/DNA complexes

100 µL of ChIP elution buffer was added to the washed and precipitated Protein A and Protein G magnetic beads as well as the input control. The samples were then incubated for 15 min at room temprature with 1000 rpm shaker. The magnetic separator was used to pellet the beads and the supernatant was transferred to a new tube. This step was then repeated once and combined supernatant form each step.

2.4.8 Reverse crosslink of protein/DNA complexes to free DNA

The samples were incubated for a further 6 hr at 65˚C to revere-crosslink. After each tube warm to room temprature 1 µL of 10 mg/mL Ribonuclease A (RNase A) added and incubated 30 min at 37˚C with 1000 rpm shaker. For degradation of crosslinked proteins, 3 µL of 20 mg/mL Proteinase K (Ambion) added to each tube and incubated a hour (hr) at 55˚C with 1000 rpm shaker.

2.4.9 DNA purification

DNA purification procedure was carried out using Zymo DNA Clean and Concentrator Kit. All the reagents used were provided by the kit unless otherwise stated.

1000 µL of DNA Binding Buffer was added to each 200 µL of the supernatant. The sample was then transferred to a spin filter in collection tube and centrifuged for 60 sec at 17000 x *g*. The flow-through in the collection tube was discarded and 200 µL

of Wash Buffer was added to the spin filter in the collection tube. The sample was centrifuged at 13000 x *g* for 60 sec. This wash was then repeated once. The flow-through was discarded and the spin filter column was centrifuged for a further 60 sec at 13000 x *g*. The spin filter was then transferred to a clean collection tube and 16 µL of Elution Buffer was added directly to the centre of the spin filter membrane. After 10 min at room temprature and 5 min 55˚C. The column was centrifuged for 60 sec at 17000 x *g*. The purified DNA was then either used immediately for analysis or stored at -20˚C.

2.4.10 Antibodies used for ChIP

All antibodies used are listed in Table 2.1.

Table 2.1: Antibodies used for ChIP.

Antibody	Amount used per IP (µg)	Source	Catalog Number	Lot Number
Anti-H3K9me3	5	Abcam	Ab8898	GR1102587-1
Anti-H3K4me3	3	Millipore	07-473	2459618
Normal Rabbit IgG	0.75 or 1	Millipore	PP64B	2013079
Anti-RNA Pol II	3 or 5	Abcam	Ab26721	GR146339-1 GR146339-2

2.4.11 Quantitative real-time PCR (qPCR) prior to ChIP-Seq

Quantitative real-time PCR (qPCR) was performed to verification of the enriched ChIP DNA. qPCR was carried out with ChIPed and input DNA on a The Applied Biosystems® StepOne™ Real-Time PCR Systems. SYBR® Green master mix (Life Sciences) was used as the method of detection in this study. GAPDH primers (amplicon size is 226 bp) was provided by The TaqMan GAPDH Control Reagents (P/N 402869) and used as a internal control primers, which housekeeping gene and therefore, should be expressed in all cell lines.

qPCR reactions were carried out in a total volume 10 µL containing 5 µL SYBR green master mix, 2 µL of 5-fold diluted purified ChIP DNA, 0,5 µL of primer mix (10 µM), 2,50 µL sterile water. QPCR conditions were used recommended by Life Sciences: 95°C for 10 min; 40 cycles of 95°C for 15 min, 60°C for 1 min, 95°C for 15 sec. PCR products were loaded on a 1% agarose gel and run at 100V for 40 min. Bands were identified under UV light.

2.5 Coupling ChIP to Deep Sequencing (ChIP-Seq)

All standard protocols for Illumina sequence preparation, quality control and sequencing were provided by Department of Genetics/ Biopolymers Facility, Harvard Medical School, USA.

2.5.1 Library preparation

2.5.1.1 DNA library preparation

The preparation of ChIP-Seq DNA libraries for Illimuna HiSeq 2500 was started from the point of purified and properly prepared DNA. Prepared library was run to confirm the concentration and size distribution of the final product using a KAPA Library Preparation Kit.

For adapter preparation, fragmented DNA samples were quantified using a NanoDrop™ spectrophotometer. Transferred 15 µl of diluted, fragmented DNA into the appropriate tube. After transferred the calculated volume of the correct adapter stock solution (Table 2.2) into each of the tubes, adjusted the volume in each tube up to 15 µl with PCR-grade water, mix well and placed on ice. Then reagents were prepared for End Repair, A-Tailing and Ligation as; a master mix (buffer and enzyme) is prepared for Ligation, while End Repair and A-Tailing Buffers and Enzymes are prepared separately. Each mix distributed into each tube 15 µl, 15 µl, 5 µl, 15 µl, respectively. Then, added 5 µl of KAPA End Repair Enzyme Mix into each of the tubes. Instrument was initiated after the deck was prepared followed by Apollo 324™ protocol.

Table 2.2: Reagents for library preparation.

Machine Block		
Block 1	**Block 2**	**Block 3**
70% EtOH (800 µL)	Fragmented DNA samples x8 (15µL)	2X Ligation Master Mix (5 µL Ligase, 6 µL 5X Buffer, 4 µL H2O)
Water wash (600 µL)	AMPure XP(200 µL)	2X Adapter Master Mix (15 µL)
Elution (600 µL)	Product Collection (15 µL)	
	ER Enzyme (5 µL)	
	3X ER Buffer (4.5 µL 10X Buffer, 10.5 µL H20)	
	AT Enzyme (3 µL + 2 µL H2O)	
	3X AT Buffer (4.5 µL 10X Buffer, 10.5 µL H20)	

2.5.1.2 Sample preparation

For confirmed the size distribution of each prepared final libraries electrophoretically, using an Agilent Bioanalyzer or TapeStation instrument. Reaction was set as; 2 µL sample/ladder and 2 µL marker. There was no high size cut off selection, only a ~100 bp low size cut-off selection was generated for ChIP-Seq.

2.5.2 Quantify libraries by qPCR

In addition, qPCR assay was run for assessing library functional concentration prior to the sequencing process using the KAPA Library Quantification Kit (for Illumina® platforms). Appropriately prepared samples with standart protocaol, 15 µL of master mix which include Kapa – 10 µL, H2O – 3,8 µL, Forward Primer – 0,4 µL, Reverse Primer – 0,4 µL, Rox HIGH – 0,4 distributed in each tube and they placed in qPCR machine. Data was generated automatically by qPCR machine.

2.5.3 Next generation sequencing (NGS)

Final DNA libraries were validated and sequenced at 50 bp per sequence read, using an Illumina HiSeq 2500 instrument, cBot clustering in one individual lane for 50 cycle runs, 50 bp single-end, rapid run within 1 day followed by standard protocol. Image analysis and base calling were performed using the HCS 1.5.15.1 software (Illumina) for HiSeq 2500.

2.5.4 Bioinformatic analysis of ChIP-Seq

Obtained ChIP-Seq data was dowloaded from website of facility and loaded ‘Galaxy’ software for analysis.

2.5.4.1 Quality control

Analysis began by loading the sequenced tags for whole ChIP-Seq datasets to ‘Galaxy’ software and converting fastqsanger format. To determine the quality of data, quality control analysis was performed by ‘FastQC’ tool in Galaxy for all datasets. FastQC parameters checked according to basic statistics, sequence quality, per sequence quality score, sequence content, GC content, N content, sequence lenght distribution, sequence duplication levels, overrepresented sequences, Kmer content. Basic statistic include general information about data which are file name, file type, encoding reagent, total sequences, filtered sequences, sequence lenght and %GC. Sequenced performed one Illumina Hiseq 2500 flow cell lane at depth of

177,447,268 sequences in total. Also, in order to check of quality of data, 'NGS: QC and manipulation' > 'Filter FASTQ' and 'FASTQ Summary Statistics by coloumn' tools in Galaxy were used.

2.5.4.2 Alignment of reads and quality control

After quality control of datasets, short sequencing reads aligned to the reference sequence by 'Bowtie2' in Galaxy using default parameter which are single-end, human reference genome (Homo sapiens) (b37): hg19. After mapping step, aligned reads checked according to quality score. Duplicate reads (multiple identical copies) were removed from mapped reads using 'NGS: SAM Tool' > rmdup remove PCR duplicates' tool in Galaxy. BAM file that was created by Bowtie 2 converted to BED files detailing the genomic coordinates of each tag for visualization of aligned reads.

2.5.4.3 Peak calling

For enriched-region (peak) identification (peak calling) of aligned reads was used two different tool algorithms which are MACS version 1.0.1 and SICER version 0.0.1 in Galaxy with 'input' data as a control sample. Actually, two of them can be used for ChIP-Seq analysis. However, MACS usually used for transcription factor description, SICER used for histone modifications.

The files which include aligned short reads was loaded the MACS and SICER software to determine enriched H3K9me3 and H3K4me3 peaks with input sample as control and algorithms as shown Table 2.3 and Table 2.4. Output of SICER intervals files were converted to BED format.

Table 2.3: MACS algorithms for H3K9me3 and H3K4me3 histone modifications.

MACS Parameters	Data	
	H3K9me3 (broad peak)	H3K4me3 (sharp peak)
-end type	single-end	single-end
Genome size	2.7e+9	2.7e+9
Tag size	50	50
Bandwith	300	300
p-value	1e-5	1e-5
MFold	32	32
Local lambda	1000-5000-10000	1000-5000-10000
Model	No	yes
Shift size	100	-

Table 2.4: SICER algorithms for H3K9me3 and H3K4me3 histone modifications.

SICER Parameters	Data	
	H3K9me3 (broad peak)	H3K4me3 (sharp peak)
Window size	200	200
Fragment size	150	150
Effective genome fraction	0,74	0,74
Gap size	600	200
Treshold value	0.01	0.01

2.5.4.4 Detection of differantial binding sites

To detect intervals with overlap and no overlap (peaks number and region on the genome) between histone marks as well as study groups, 'Operate Genome' > 'subtract region' and 'intersect region' tools in Galaxy were used with at least 1 bp default. Also, common peaks in MACS and SICER was determined with 'Intersect the intervals of two datasets' in Galaxy for a histone marks.

2.5.4.5 Gene ontology analysis

For the pathway analysis, Gene Ontology (GO) analysis was done using 'DAVID' software. DAVID analyses were performed online using defaults parameters which are treshold=2, EASE=0,1, Benjamini for GO enrichment analysis for overlapping genes in H3K9me3 and H3K4me3 histone modifications.

2.5.4.6 Peak annotation and visualization

The BED files include enriched peaks location on chromosome with coordinates and they were annotated to reference geneome (hg19) using 'PAVIS' and 'Nebula' softwares are accessible online within relavent genomic region. Annotated peaks were displayed by USCS Genome Browser and IGV tool.

2.6 Validation of ChIP-Seq Data by ChIP-PCR

2.6.1 Primer designing

For ChIP analysis with PCR primer parameters are important and selected based on primer length (20-24 bp), product size (80-200 bp), melting temperature (Tm: 59-60˚C), GC content (40-60%). GAPDH primers sequences were obtained from EZ-ChIP Kit (Millipore) which used as a positive control primers. Primers designed for amplification of exon 1 and promoter region in MEFV, exon 3 region in NLRP3 and

exon 2 region in TNFRSF1A. Appropriate and spesific primers to the gene of interest were designed using Primer-Blast tool as described in Table 2.5.

Table 2.5: Primer parameters.

Primer name	Strand	Sequence (5'>3')	Tm (˚C)	%GC	Amplicon Size
MEFV exon 1	F	ACGGCGTACTCTTCCCCATA	60.40	55.00	192 bp
	R	GACCCCTAGTGACCATCTGC	59.53	60.00	
MEFV promoter	F	GGCAGGTTGTGAAATAGCGG	59.55	55.00	85 bp
	R	CATGGACACACCCTTACCCTT	59.65	52.38	
GAPDH	F	TACTAGCGGTTTTACGGGCG	60.18	55.00	166 bp
	R	TCGAACAGGAGGAGCAGAGAGCGA	67.02	58.33	
NLRP3 exon 3	F	TTCTCCATTCCGGTTACCAC	59.79	50.00	592 bp
	R	TTCTGGAGGGTTTTCTCACG	60.22	50.00	
TNFRSF1A exon 2	F	AGGACTTGAGCCAGGGAAGT	60.25	55.00	397 bp
	R	GCCGATTCCCTGAAGTCTCT	60.73	55.00	
Negative primer	F	ATGGTTGCCACTGGGGATCT	61.22	55.00	174 bp
	R	TGCCAAAGCCTAGGGGAAGA	60.84	55.00	

2.6.2 Primer optimization

Human GAPDH (166 bp), MEFV (exon 1 and promoter), NLRP3 (exon 3), TNFRSF1A (exon 2) and negative control primers were optimased using genomic and sonicated DNA with different annealing temperatures by gradient PCR. In addition, primers optimased with different concentration as a final concentration is 0,2 μM, 0,4 μM, 0,8 μM with genomic and sonicated DNA. In this step, all PCR reaction carried out on Bio-Rad T100™ Thermal Cycler. PCR reaction was set as; 0,3 μL for 2 U/μL Q5® High-Fidelity DNA Polymerase (BioLabs), 5 μL for 5X Q5 Reaction Buffer (BioLabs), 5 μL for 5X Q5 High GC Enhancer (BioLabs), 0,5 μM for dNTP (10 mM) 1 μL for template (50 ng/μL), 1 μL for primers (10 μM) and added sterile water up to 25 μL. PCR conditions were set as described Table 2.6. Then, PCR prodcuts were analysed by gel electrophoresis.

Table 2.6: PCR conditions.

Step	Temperature (ºC)	Time	Cycle number
Initial denaturation	98	30 sec	1
Denaturation	98	10 sec	35
Annealing	58-62 (GAPDH) 60-65 (TNFRSF1A, NLRP3) 61-64 (MEFV) 60-70 (negative control)	30 sec	35
Extension	72	30 sec	35
Final extension	72	7 min	1
Hold	12		

2.6.3 ChIP-PCR

We was detect that enriched region (approximately 1600 bp length) by SICER and MACS (FDR<0,01 and Mfold:32) using input control in MEFV gene as a result of ChIP-Seq. For confirmation of ChIP-seq peaks, we carried out PCR with 10 ng of ChIPed DNA and input that the exactly same as the sent samples to high throughput sequencing. In addition to MEFV and GAPDH, two genes of the binding targets which are NLRP3 and TNFRSF1A, selected randomly to validate the H3K9me3 and H3K4me3 ChIP sequencing data by PCR. In addition, PCR validation was performed in individual samples; 3 FMF patients during attack period, the same 3 FMF patients during attack-free period and 3 healthy subjects. PCR reactions and conditions were set up as described in Table 2.6 with 60°C, 62°C and 64°C annealing temperature for GAPDH, NLRP3 and TNFRSF1A, MEFV and negative control primers, respectively. PCR prodcuts were analysed by electrophoresis on 1% agarose gel.

RESULTS

3.1 PBMCs Isolation from Whole Blood

As MEFV gene expression higher in white blood cells, patients and healthy group PBMCs were isolated from pheripheral blood by density gradient. Collected PBMCs from on histopaque solution were counted via hemocytometer. Isolated PBMCs number from all study groups shown in Table 3.1.

Table 3.1: PBMCs numbers of study groups.

Sample	PBMCs number/ ml		
	FMF patients during attack	FMF patients during attack-free	Healthy control
1	2500000	700000	2000000
2	2000000	1550000	1500000
3	1150000	1000000	1250000
4	700000	1200000	1750000
5	1400000	1000000	1000000
6	1000000	1300000	1000000
7	500000	700000	5000000
8	1000000	500000	2000000
9	1500000	110000	2000000
10	5000000	1000000	2500000

3.2 Chromatin Fragmentation to Short Pieces

3.2.1 Cell lysis buffer (SDS) optimization

For disrupt of nuclear membrane to dispose protein and chromatin, cell lysis buffer (SDS) was used before crosslinking. Cell lysis buffer include SDS detergent and its concentration important for efficiency of buffer. Cell lysis buffer including 1% and 0,25% SDS was used to optimisation of SDS concentration with same amount of cell. DNA purified with spin-coloumn after protein digestion and measured via Nanodrop. Efficient SDS concentration that creates high amount of DNA was found as 1% and used for ChIP assay as described in Table 3.2.

Table 3.2: SDS concentration optimization.

Concentration of SDS	Volume/Cell number	DNA amount
1%	1 mL / $1x10^7$	28,4 ng/µL
0,25%	1 mL / $1x10^7$	20,4 ng/µL

3.2.2 Sonication optimization

The aim of the sonication step is to shear the chromatin into small fragments without damaging the DNA-binding proteins. Keeping proteins without damage, should be ensure about efficiency of fixation. Chromatin length directly effects the resolution of the ChIP. Also, the smallest fragment of chromatin without damaging the nucleosome is around 200 bp, it can be said histone modification was most bound nucleosome. However, too short fragment may create suspection about the target regions localisation, because of nucleosome nearly 147 bp. Therefore, the aim is generate 200-700 bp fragments with most of 300-500 bp. To check of sonication efficiency, purified DNA was analysed by agarose gel electrophoresis after reverse-crosslink. The sonicated samples appear as a smear on the gel with different size DNA as shown Figure 3.1.

To optimase of sonication conditions, HL-60 cell was used on a Bandelin Sonoplus Sonicator with MS-72 probe on ice. Different settings was tried for example power, pulse number, pulse and stop time with same initial amount of cells as described in section 2.4.2.3. The length of fragments between mostly 200-700 bp was created with 20 cycles (30 sec on/ 30 sec off), 30 W sonication conditions on ice (Figure 3.1). But, other trials did not create desired DNA smear on gel.

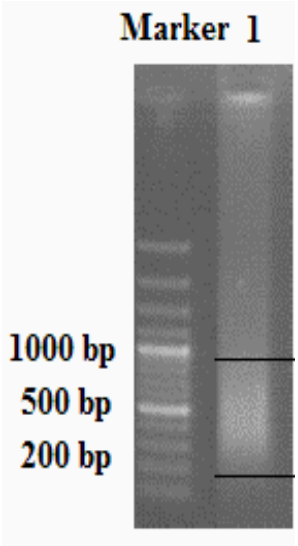

Figure 3.1: The fragmented DNA (Lane 1: sonicated DNA for 20 min).

3.2.3 Fragmented chromatin

Sonication performed in order to fragmentation of crosslinked DNA until reach to 200-700 bp lenghts. Purified DNA lenght checked with 1 or 2 % agarose gel, 90 or 100 V for 40 min and visualized under UV light after reverse-crosslink. If fragments were bigger than expected, sonication process was repeated. Most parameters directly effect fragmentation of DNA in cell lysis buffer such as volume, density, temprature, type of tube used. Nearly all sample were sheared 200-500 bp length fragments, as a shown in Table 3.3. This result indicate that, samples are suitable for chromatin immunoprecipitaton assay.

Table 3.3: Sonicated chromatin length.

Sheared DNA (bp)			
Sample	**FMF patients during attack**	**FMF patients during attack-free**	**Healthy control**
1	200-500	300-600	200-400
2	200-500	200-500	200-600
3	200-1500	200-800	150-1000
4	200-500	200-800	150-1000
5	200-500	200-500	250-800
6	300-600	300-600	250-800
7	200-600	200-400	200-800
8	200-500	200-400	150-800
9	300	200-500	150-1000
10	200-400	200-700	150-1000

3.3 Chromatin Immunoprecipitation (ChIP)

3.3.1 Antibody binds to magnetic beads

In ChIP, antibody firstly bind to magnetic beads, then antibody/bead complex interact with fragmented chromatin in cell lysate. The aim is show that antibody interaction with magnetic beads via western blotting. 2 µg of RNA pol II antibody incubated at +4°C for 2 hr with magnetic beads, then eluted with 100 µL glycine solution for two times. According to western blotting, RNA pol II antibody was able to intact to magnetic beads (Figure 3.2).

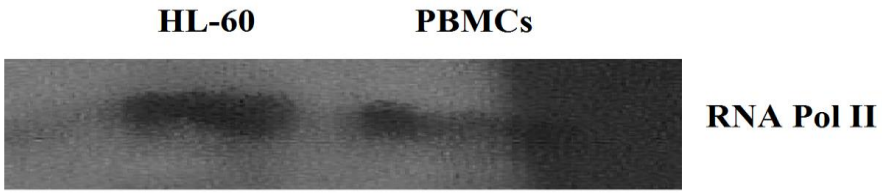

Figure 3.2: Antibody binds to magnetic beads.

3.3.2 Immunoprecipitation

Immunoprecipitation carried out with rabbit polyclonal H3K9me3, H3K4me3, Normal IgG and RNA Pol II antibodies in PBMCs of FMF patients (attack and attack-free period) and healthy control. After immunoprecipitation, reverse-crosslinked DNA that presents protein binding sites was purified and measured concentration by Nanodrop (Table 3.4).

Table 3.4: Enriched DNA concentration.

	FMF patients during attack			FMF patients during attack-free			Healthy control		
Sample	**H3K9me3** (ng/µL)	**H3K4me3** (ng/µL **)**	**input** (ng/µL)	**H3K9me3** (ng/µL)	**H3K4me3** (ng/µL**)**	**input** (ng/µL)	**H3K9me3** (ng/µL)	**H3K4me3** (ng/µL)	**input** (ng/µL)
1	7,8	17	15,7	37,6	56,6	18,4	208,7	54,9	31
2	85,4	10,9	38,9	53	19,8	20,1	119,7	38,6	12,6
3	33,6	11,7	12,7	16,2	9,2	9,4	80,9	102,1	58,2
4	60,9	22,6	34,5	24,6	20,2	12,8	98	68,9	64,4
5	98,5	31,2	58,8	76,5	23,5	25,8	48,4	91,1	70,6
6	135,8	51,4	73,3	79,3	20,1	143,7	126,4	55,6	28,8
7	117,6	49,7	49,4	20,1	20,1	39,6	61,5	49,6	78,1
8	14,6	29,1	37,2	42	54,7	11,9	83,8	78,2	89,2
9	120,9	84,8	79,3	276,7	217	42,4	43,6	5,5	16,6
10	46,1	24,2	31,5	291,8	60,8	55,3	80,4	85	22,5

3.3.3 ChIP validation with qPCR

Quantitative real-time PCR (qPCR) was performed to verification of the enriched ChIP DNA with housekeeping primers (GAPDH) and Ct values were analysed manuallly or IPs and input control based on the input DNA fraction Ct value should be ≤30 and Ct [mock] – Ct [ChIP] > 1.0 to be considered quantitatively above the background signal (noise) for the sample. Also, PCR product were analysed by electrophoresis on a 1% agarose gel and visualized under UV light. ChIP performed with the RNA Pol II antibody was greatly enriched (Figure 3.3) based on qPCR analysis. Then, samples were prepared for deep sequencing; ChIPed DNA diluated to final concentration is 10 ng/µL, pool each group and half of them sent to sequence, remaining ChIPed DNA kept -20°C.

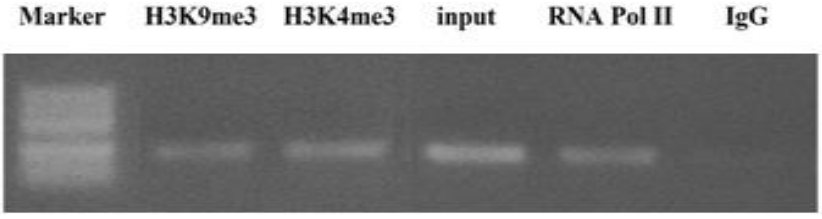

Figure 3.3: qPCR bands with GAPDH primers of IP and input samples of FMF patients during attack period.

3.4 Chromatin Immunoprecipitation Sequencing

3.4.1 Quality control of ChIPed DNA prior to NGS

Fragmented DNA samples was prepared for high throughput sequencing and DNA fragments length checked via TapeStation system. As a result of Bioanalyser fragments length was found as average 300-600 bp (Figure 3.4). After library preparation step quality control applied by qPCR. This data suggests that our libraries were successfully created and have sufficient sample with the pH:5 and pH:7 regions to bind to the flow cell and successfully produce clusters for sequencing (Table 3.5).

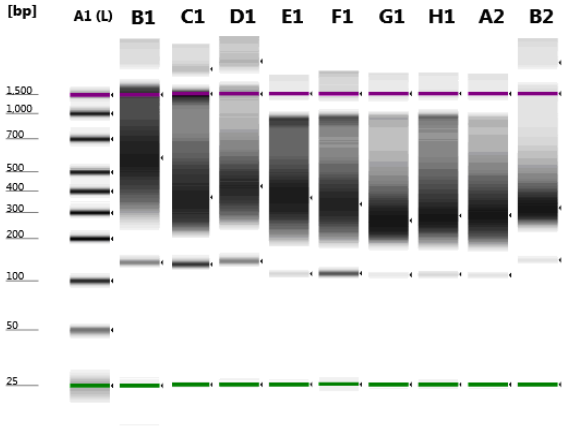

Figure 3.4: Smear of fragmented DNA samples (A1: Marker; B1, E1, H1: H3K9me3; C1, F1, A2: H3K4me3; D1, G1, B2: input).

Table 3.5: DNA libraries concentration prior to NGS.

Histone Modification	Study Group	Concentration
H3K9me3	FMF-attack	750 nM
	FMF-attack free	743.75 nM
	Healthy control	329.72 nM
H3K4me3	FMF-attack	225.5 nM
	FMF-attack free	251.6 nM
	Healthy control	274.66 nM
Input	FMF-attack	454.73 nM
	FMF-attack free	329 nM
	Healthy control	429.12 nM

3.4.2 ChIP-Seq data

After DNA library preparation and sequencing, ChIP-Seq data was generated and loaded website 'Biopolymers Facility' by Harvard Medical School, Biopolymers Facility at a depth of approximately 177 million sequences and about 7.5 Gigabyte size in total. Data was dowloaded from this website and loaded 'Usegalaxy' software for analysis.

3.5 Bioinformatic Analysis of ChIP-Seq

3.5.1 Quality control report of raw data

According to FASTQC results, total sequence number of each data was different. Defaults of sequence lenght is 50, per sequence quality score is higher than 30 which are most important for reproducibilty of datasets. Also, in order to check of quality of data, 'NGS: QC and manipulation' > 'Filter FASTQ' and 'FASTQ Summary Statistics by coloumn' tools in Galaxy were used. It was determined no differenties reads number after filtering with default is less than 30 quality score and sequence length is 50 (Table3.6 and Figure D.1). This result show that we have high quality data for bioinformatic analysis.

Table 3.6: Reads number and their quality score.

Histone Modification	Study Group	Total Read	Read Q≥30
H3K9me3	FMF-attack	9780374	9780374
	FMF-attack free	9672826	9672826
	Healthy control	14964546	14964546
H3K4me3	FMF-attack	12882346	12882346
	FMF-attack free	15713665	15713665
	Healthy control	21612517	21612517
Input	FMF-attack	11692069	11692069
	FMF-attack free	24428624	24428624
	Healthy control	22440665	22440665

3.5.2 Aligned data to reference genome

Bowtie2 tool creates two BAM format files include aligned (unique and multiple alignments) and unaligned reads. This data show that higher than 73% of reads aligned to human genome (hg19) and higher than 54% was uniquely aligned to human genome (hg19) of these reads. Bowtie2 results show that H3K4me3 coverage

higher than H3K9me3 histone modification. Furthermore, input coverage higher than the two histone modifications as expected (Table 3.7). Also, we detected alignments on the MEFV gene for both of histone modifications in all study group.

Table 3.7: Mapped reads summary.

Histone Modification	Study Group	Mapped Reads	Uniquely Mapped Reads and Percentage	Multi-mapped Reads and Percentage	Non-mapped Reads and Percentage
	FMF attack	9780374	5451356 (55.74%)	2322428 (23.75%)	2006590 (20.52%)
	FMF attack-free	9672826	6127991 (63.35%)	2392419 (24.73%)	1152416 (11.91%)
H3K9me3	Healthy control	14964546	9215623 (61.58%)	3946864 (26.37%)	1802059 (12.04%)
	FMF attack	12882346	7111614 (55.20%)	2403135 (18.65%)	3367597 (26.14%)
	FMF attack-free	15713665	9126020 (58.08%)	3233930 (20.58%)	3353715 (21.34%)
H3K4me3	Healthy control	21612517	14536683 (67.26%)	4989389 (23.09%)	2086445 (9.65%)
	FMF attack	11692069	6400004 (54.74%)	2545010 (21.77%)	2747055 (23.50%)
	FMF attack-free	24428624	16538216 (67.70%)	5864971 (24.01%)	2025437 (8.29%)
Input	Healthy control	22440665	13337599 (59.43%)	4743564 (21.14%)	4359502 (19.43%)

3.5.3 ChIP-Enriched regions

MACS and SICER tools were used for peak calling of uniquely aligned reads for both histone modification. MACS was created BED file which include chromosome ID and coordinates. SICER was generated interval format files and they were converted to BED format by BEDTools. Table 3.8 shows that peak number of created by MACS and SICER for H3K9me3 and H3K4me3 histone modifications. Peak calling result show that SICER detected lots of regions than MACS. On the other hand, peaks number of H3K9me3 modification present to inactive region was detected as significantly lower (nearly 10 fold) than H3K4me3 modification present to active region in the genome by SICER. Then, overlap peak regions between MACS and SICER for H3K4me3 and H3K9me3 detected by 'Operate Genome' > 'Intersect the intervals of two datasets' tool with at least 1 bp default (Table 3.8).

Table 3.8: Peak number and overlapping intervals of MACS and SICER.

Histone Modification	Study Group	Peak Number		
		MACS	SICER	Overlapping
	FMF attack	197	1.351	61
	FMF attack-free	132	974	56
H3K9me3	Healthy control	560	2.656	331
	FMF attack	19.114	13.373	18.886
	FMF attack-free	4.872	9.255	4.168
H3K4me3	Healthy control	8.118	10.828	7.643

3.5.4 Differential binding sites

Different and same peak regions of ChIP-Seq data in all study groups (patients and control) for H3K9me3 and H3K4me3 modificaitons were detected by Operate on Genomic Intervals tool in Galaxy. After overlap and non-overlap regions of the modifcations were detected, peaks annotated to reference genome and associated with genes (Figure 3.5).

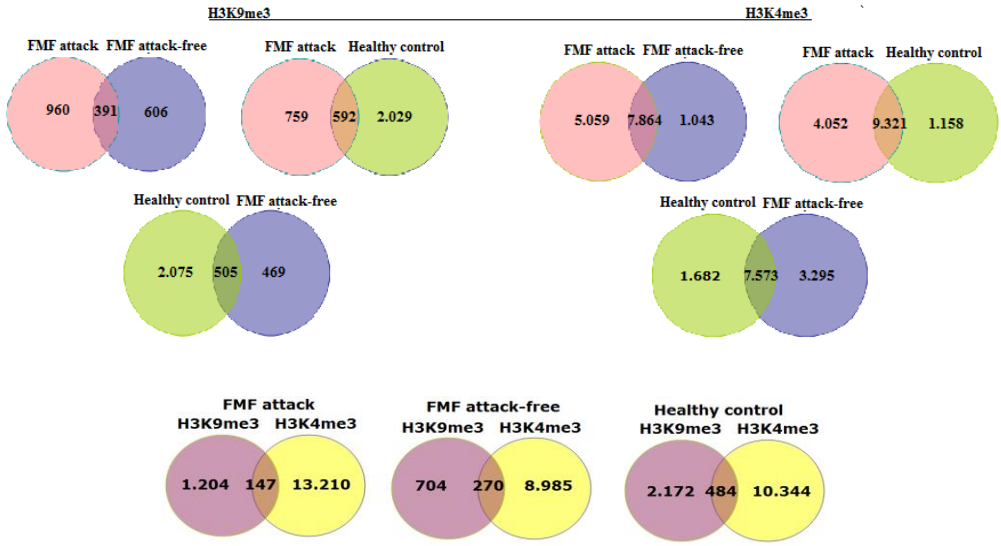

Figure 3.5: Differential binding sites of ChIP-Seq peaks.

3.5.5 Enriched biological themes

GO enrichment analysis was done for identification of overlapping genes in H3K9me3 and H3K4me3 marks. The 16 most enriched GO annotations and the numbers of genes within each annotation are listed based on DAVID (Figure 3.6).

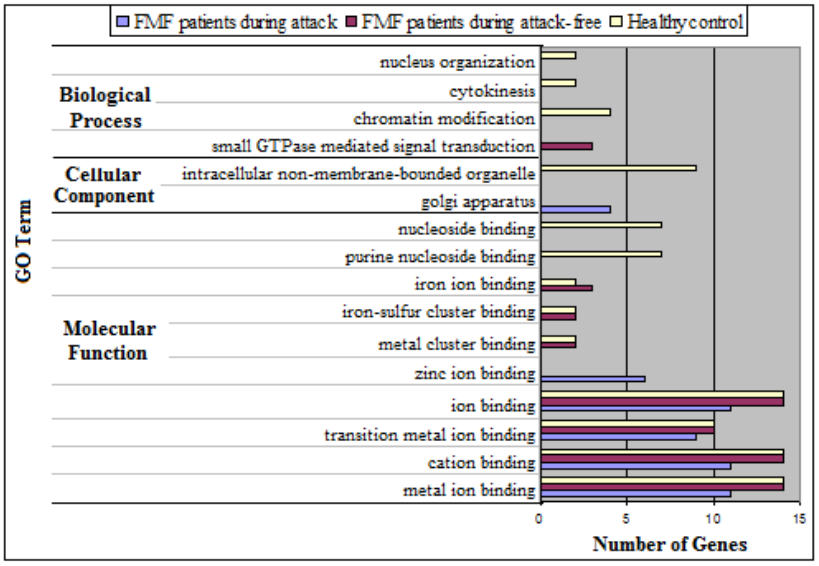

Figure 3.6: GO analysis for overlapping genes in H3K9me3 and H3K4me3.

3.5.6 Annotated peaks and visualization

ChIP-Seq peaks annotated using PAVIS and Nebula software within relevant genomic context and visualised on UCSC Genome Browser and IGV tool with manual (Figure D.2). Output of annotation includes closest gene to each peak and its relative region such as enhancer (-30000), promoter (-1000), immediate downstream (+1000), intragenic region, gene downstream (+5000), gene transcription start site (TSS) and gene body. Furthermore, genes associtated peaks generated by PAVIS and localization on the gene were provided by Nebula software. We detected that enrichment of the modifications of H3K9me3 and H3K4me3 happen mostly intragenic and regulatory regions of genome, respectively, as expected (Table 3.9 and Figure 3.7).

Table 3.9: Peak location annotation.

Histone Modification	Study Group	Number of Total Peaks	Number of Gene Associated Peaks
H3K9me3	FMF attack	1.351	421
	FMF attack-free	974	243
	Healthy control	2.656	886
H3K4me3	FMF attack	13.373	11.942
	FMF attack-free	9.255	8.051
	Healthy control	10.828	9.435

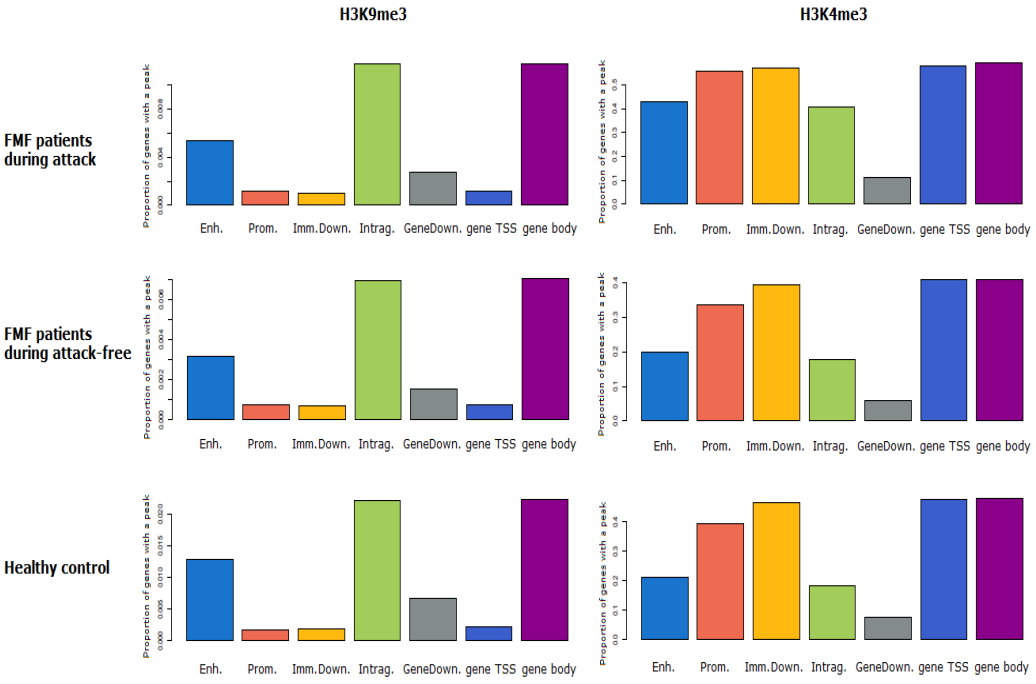

Figure 3.7: Genomic location distribution of ChIP-Seq peaks.

Then, ChIP-Seq peaks was generated in BED file format by peak caller and displayed by UCSC Genome Browser and IGV tool. Significantly enriched peak region (chr16:3305201-3306800) which are 1600 bp length and include promoter, exon 1 and part of intron 1 of MEFV gene for only H3K4me3 (p value=1.39x10^{-8}, fold change=3.40, FDR=1.77x10^{-8}) was detected in FMF patients during attack based on SICER. Also, we detcted the peak (145 bp) in the same region of MEFV (chr16:3306413-3306557) based on MACS (fold change=25.90, FDR=02,4%) (Figure 3.8). Furthermore, enriched regions by H3K4me3 modification according to FMF during attack-free period and healthy controls were detected in autoinflammation related genes at mostly promoter regions which are AP1S3, IL10RA, IL10RB, LPIN2, MVK, NLRP3, PLCG2, PSTPIP1, RBCK1, SH3BP2, SLC29A2, TMEM173, TNFRSF1A, TNFRSF11A in FMF patients during attack (FDR<0,01). Also, only H3K4me3 enriched regions (peak) were detected in pyrin related genes at mostly promoter regions which take role in inflammation pathway according to healthy controls and FMF patients during attack-free period, which are PYCARD, CASP1, HSP90AA1, NLRP3 (Table 3.9 and Figure D.3). However, it was not detected peak enriched by H3K9me3 histone modification in these genes in study groups (data was not shown).

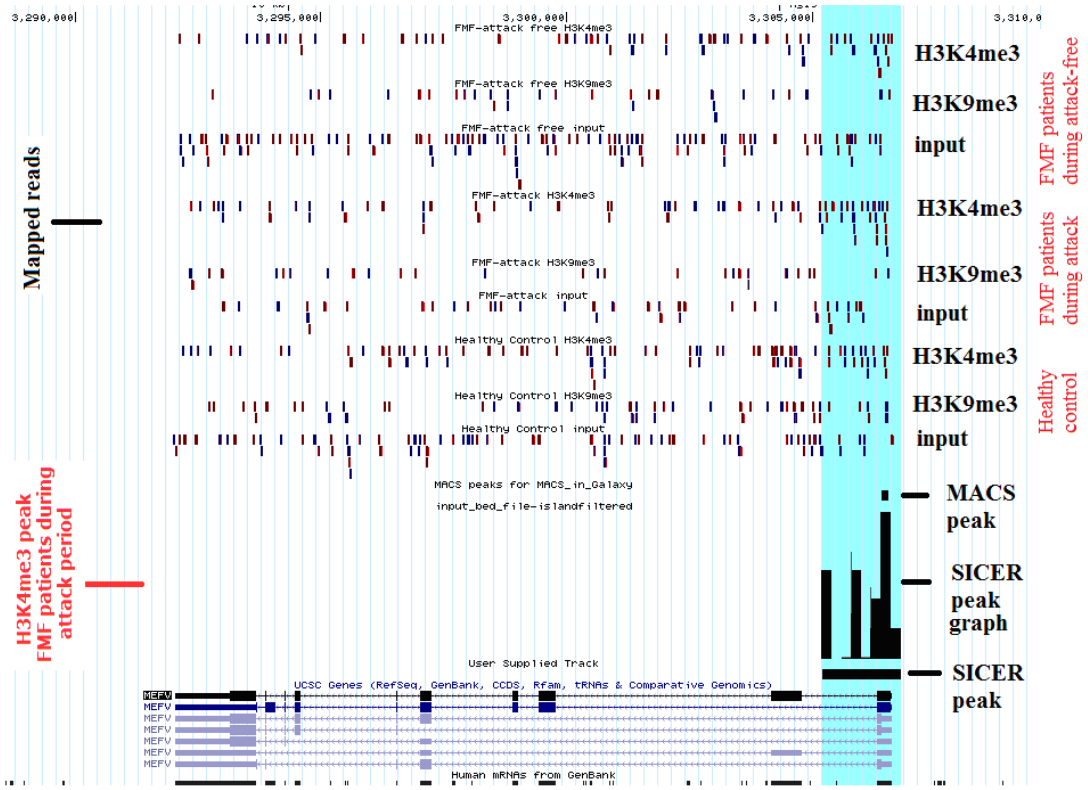

Figure 3.8: ChIP-Seq data visualization in the MEFV gene.

Table 3.9: H3K4me3 modification enriched regions feature.

	Gene ID	Gene symbol	Genomic coordinates (hg19)	Size (bp)	P value	Fold change	FDR
AUTOINFLAMMATION RELATED GENES	NM_001039569	**AP1S3**	chr2:224701401-224703400	700	2.88941983461e-17	4.76207141585	5.20521254592e-17
	NM_001558	**IL10RA**	chr11:117855801-117863200	7400	5.12319300155e-47	4.05003920654	4.86801230555e-46
	NM_000628	**IL10RB**	chr21:34638201-34640000	1800	4.9549010084e-39	10.9094726981	2.86334353063e-38
		LPIN2	chr18:3012001-3013200	1200	1.68082380586e-21	7.40285647373	3.68770196865e-21
	NM_001198536	**MEFV**	chr16:3305201-3306800	1600	1.39393836439e-08	3.40921021817	1.77029519601e-08
	NM_000431	**MVK**	chr12:110010801-110012400	1600	1.82503709948e-12	5.2599243366	2.66333122525e-12
	NM_001079821	**NLRP3**	chr1:247578601-247580600	2000	4.21927093816e-11	4.17454312429	5.84619735805e-11
	NM_002661	**PLCG2**	chr16:81812201-81814000	1800	6.2385920511e-29	8.96135257347	2.00770825625e-28
	NM_003978	**PSTPIP1**	chr15:77286601-77290200	3600	3.41537699162e-24	4.79537261456	8.49530537074e-24
	NM_006462	**RBCK1**	chr20:388001-389800	1800	5.63914219146e-23	5.96611788179	1.32626081053e-22
	NM_001122681	**SH3BP2**	chr4:2819001-2821000	2000	4.4806531092e-14	7.46779381122	6.97983429051e-14
	NM_001532	**SLC29A2**	chr11:66138401-66140200	1800	3.05509468902e-18	7.54896548308	5.77824438299e-18
	NM_198282	**TMEM173**	chr5:138860801-138862400	1600	3.78613893751e-19	7.79248049867	7.46370937163e-19
	NM_001065	**TNFRSF1A**	chr12:6448401-6452000	3600	9.50346684743e-42	6.03917238647	6.40491160741e-41
	NM_001278268	**TNFRSF11A**	chr18:59992401-59993200	800	6.9539120605e-10	7.3054504675	9.2224261118e-10
PYRIN RELATED GENES	NM_001184902	**CARD8**	chr19:48757601-48759800	2200	8.68307693999e-14	4.73114887419	1.33155984571e-13
	NM_001257118	**CASP1**	chr11:104902601-104906200	3600	2.99995150501e-20	3.95711900323	6.18865747794e-20
	NM_001017963	**HSP90AA1**	chr14:102551401-102554800	3400	2.87363528889e-63	11.2016907168	7.56732413762e-62
	NM_001271970	**HSP90AB1**	chr6:44213601-44216200	2600	5.72850853638e-48	9.37532809996	5.80753587127e-47
	NM_001079821	**NLRP3**	chr1:247578601-247580600	2000	4.21927093816e-11	4.17454312429	5.84619735805e-11
	NM_001145860	**POP1**	chr8:99128801-99130200	1400	7.91558905827e-11	3.6797824577	1.09044932654e-10
	NM_013258	**PYCARD**	chr16:31212001-31214400	2400	6.19421663722e-43	9.46229774838	4.56660853937e-42

3.6 ChIP-Seq Confirmation with PCR

3.6.1 Primer optimization

MEFV promoter and exon 1, NLRP3 exon 3, TNFRSF1A exon 2 and human GAPDH (166 bp) control primers were optimased using genomic and sonicated DNA with different annealing temperatures by gradient PCR (58-65°C). PCR product loaded on agarose gel (1%) and visualized under UV light. 64°C, 62°C and 60°C were detected as a appropriate temperature for MEFV and negative control primers, NLRP3 and TNFRSF1A, GAPDH, respectively (Figure 3.9, Figure 3.10, Figrue 3.11 and Figure 3.12). Also, primer concentration was optimased for different final concentration with genomic and sonicated DNA such as 0,2 µM, 0,4 µM, 0,8 µM. Optimum primer concentration detected as a final concentration is 0,5 µM for all primers (data was not shown).

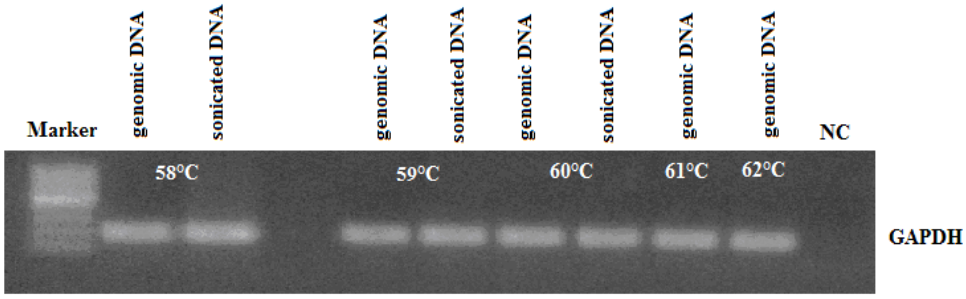

Figure 3.9: Gradient PCR with GAPDH primers. (NC: Negative control).

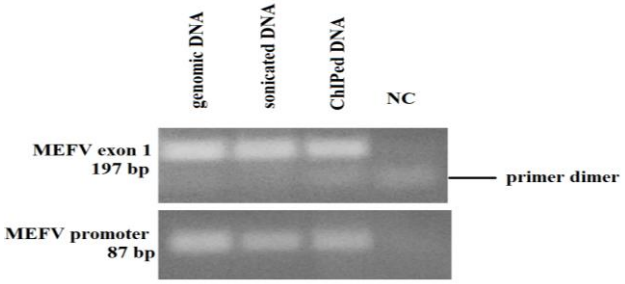

Figure 3.10: PCR with MEFV primers at 64°C annealing temperature. (NC: Negative control).

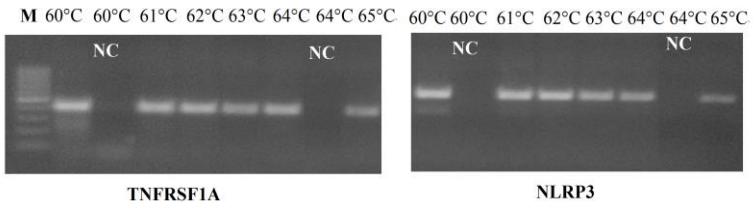

Figure 3.11: Gradient PCR with TNFRSF1A and NLRP3 primers. (M: Marker, NC: Negative control).

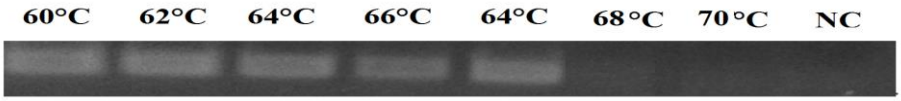

Figure 3.12: Gradient PCR with negative control primers. (Lane 1-4, 6, 7: genomic DNA, Lane 5: sonicated DNA, NC: Negative control).

3.6.2 ChIP PCR

For confirmation of ChIP-Seq results, standard PCR for MEFV, NLRP3, TNFRSF1A gene, GAPDH gene as an internal control and negative control primers were carried out in pooled and individual samples during attack and attack-free periods of FMF patients with healthy controls. We were confirmed the signals from both modification in ChIP samples as seen in Figure 3.13 and Figure 3.14. However intentisities of the bands can not be correlated with ChIP-Seq for which the possible reasons are discussed below.

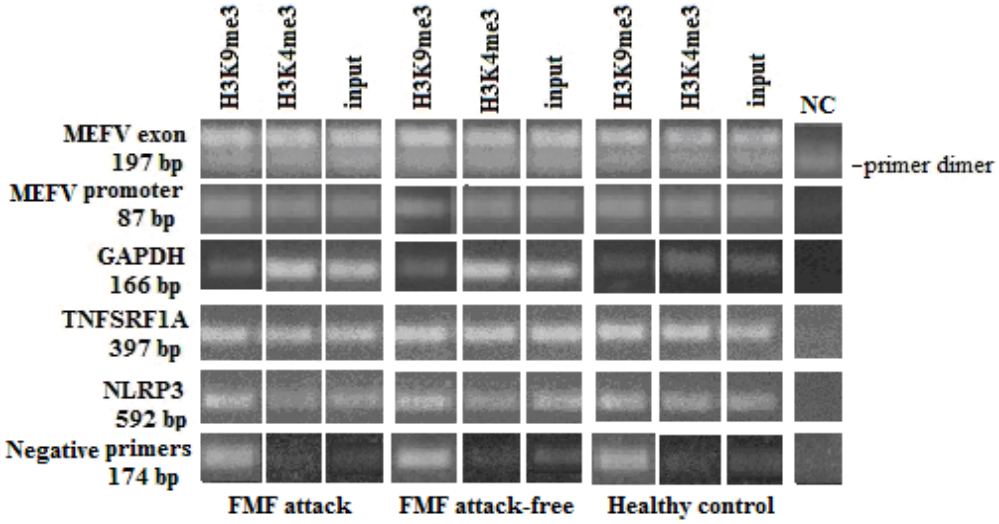

Figure 3.13: PCR confirmation of ChIP-Seq peaks in pooled samples. (NC: No DNA control).

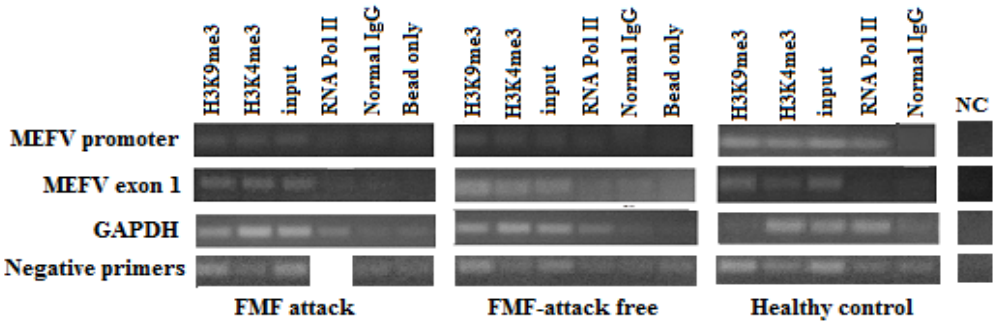

Figure 3.14: PCR confirmation of ChIP-Seq peaks in individual samples. (NC: No DNA control).

4. DISCUSSION

To date, more than 200 FMF-associated mutations have been detected in the MEFV gene (Menthie`re, 2003). However, MEFV mutations are also observed in non-FMF conditions such as Behçet Disease (Touitou et al., 2000), Rheumatoid Arthritis (Touitou, 2001) and Crohn's Disease (CD) (Fidder et al., 2005). These evidences have urged that MEFV may be a general inflammatory response gene rather than specific only for FMF disease. Furthermore, presence of FMF patients that do not carry any mutation in the MEFV gene (Ben-Zvi et al., 2015), increased MEFV exon 2 methylation (Kirectepe et al., 2011a) and exon 2 deleted alternative splice transcript (Kirectepe et al., 2011b) suggested us to explore the chromatin dynamics of the FMF patients.

Through post-translational modifications of histone tails, chromatin structure can be either a closed or open structure (Rosenfeld et al., 2009). Depending on its location, histone methylation may be a marker of active or inactive regions of chromatin (Wilson, 2008). Trimethylation of histone H3 lysine 9 (H3K9me3) is a mark associated with gene repression, and trimethylation of histone H3 lysine 4 (H3K4me3) mark is linked to active transcription and thus, gene expression (Barski et al., 2007). H3K4me3 mark is associated with CpG-rich promoters regardless of their transcriptional activity (Guenther et al., 2007; Mikkelsen et al., 2007). Functional connections between 5 hydroxymethyl cytosine (5hmC) and histone lysine methylation have been identified, by the discovery that UHRF1 and MeCP2 can also bind to 5hmC (Rose and Klose, 2013). So, histone lysine methylation and DNA methylation do not act independently. Although histone marks are associated with transcription initiation and transcription repression, such as H3K4me3 and H3K9me3, respectively, they also can be associated with splicing gene-specifically (Podlaha et al., 2004).

In order to explore post-transcriptional process of MEFV, its relation with DNA methylation and inflammation status, we carried out chromatin immunoprecipitation experiment with specific antibodies againts to H3K9me3 and H3K4me3 modifications, normal IgG as a negative control and RNA Pol II as a positive control

in peripheral blood mononuclear cells (PBMCs) of FMF patients during attack and attack-free time and healthy volunteers. ChIP assay coupled by next generation sequencing (ChIP-Seq) to identification genome wide regions occupied by chromatin associated target proteins.

PMBCs were collected form all individual because of high expression of MEFV and their amount showed differenties for all individual, revealed increased number in FMF patients during attack period compared to FMF during attack-free period as a results of inflammation. Size of fragmented chromatin is a major event that effect ChIP resolution, too short fragment (less than 200) may create suspect about target regions localisation, because of nucleosome nearly 147 bp. Conditions vary with sonication device and probe size used, volume and concentration of sample, type of tube used, pulse power and time. For efficient fragmentation, we preferred to sonication at low power, in combination with several pulses, chromatin sample cooled on ice during sonication and avoid foam as a result of presence of detergent (SDS) in the sonication buffer. After this step, created cell lysate can stored -80°C for several months. In immunoprecipitation (IP) step, positive control antibody, no antibody or normal IgG as a negative control and input control which represent to started material should be used to ensure the reliability of ChIP data. Also, all antibodies should be ChIP-grade. But generally, normal IgG control results in false positive background because of unspecific binding and antibody sensitivity. We used polyclonal antibody because its may recognize several epitopes of the target, increasing signal levels of low-abundance templates (Haring et al., 2007). As a limitation of ChIP, we get little amount of enriched DNA. However, ~10 ng of ChIP enriched DNA enough for ChIP-Seq analysis. ChIP-Seq experiment yield several million short nucleotide sequences corresponding to the possible binding sites of a given protein. In order to deeper sequence of DNA, narrow factor (H3K4me3) 20 million reads may be adequate and broader factor (H3K9me3) require more reads, up to 60 million in mammalian ChIP-seq (Bailey et al., 2013). In our experiment, we get 13-22 million reads for H3K4me3, 10-15 million reads for H3K9me3 and 12-25 million reads for input control which should be higher than ChIP samples, 177,447,268 in total from one lane of HiSeq 2500 machine. So, our experiment may not be enough for variations analysis of especially H3K9me3 broad marks for all

genome, this experiment should be repeated with higher number of reads for deeper sequence.

Bioinformatic analysis of ChIP-Seq revealed that higher than 73% of short reads aligned to human reference genome (hg19) with 54% of these was uniquely mapped and input coverage higher than two target modification as expected. For peak calling, input was used as a control that provide evaluation of p value, fold change and false discovery rate (FDR) of enriched sample according to starting material. As a result of peak calling, we detected that H3K4me3 active mark coverage nearly 10 fold higher than H3K9me3 inactive mark (p=0.076). Most of enriched regions according to input control expanded of regulatory regions for H3K4me3 and intragenic regions for H3K9me3. In this step, peak caller algorithms is most important for detection of real enriched regions for example, window size, gap size, threshold FDR value and show differenties according to peak types. In MEFV that is our primary target gene, we detected that alignments of reads in all sample for both marks but enriched regions (peak) were detected for only H3K4me3 mark in FMF patients during attack according to input control (p value $=1.39x10^{-8}$, fold change=3.4), which include promoter, exon 1 and part of intron 1 (1600 bp) of MEFV as expected from H3K4me3 mark.

Overlapping and non-overlapping intervals of H3K9me3 and H3K4me3 peaks in all study groups were detected using PAVIS software and gene ontology enrichment analysis for overlap genes was performed using DAVID softtware. Also, we were chosed randomly autoinflammation disease and pyrin inflammation pathway related genes for realize relation of these with histone modification, MEFV and/or inflammation. Peak calling analysis revealed that whereas no enrichment of H3K9me3 mark, H3K4me3 mark showed meaningful peak in most target genes in FMF patients during attack and attack free period or healthy control, but some of them showed enrichment in only FMF patients during attack period according to input control which are AP1S3, IL10RA, IL10RB, LPIN2, MVK, NLRP3, PLCG2, PSTPIP1, RBCK1, SH3BP2, SLC29A2, TMEM173, TNFRSF1A, TNFRSF11A, PYCARD, CASP1, HSP90AA1, NLRP3 (FDR<0.01). These results suggested us to, post-translational histone modifications may associated with increased DNA methylation via contribute to these epigenetic process in FMF patients. Moreover, H3K4me3 modification may has a role in progression of inflammation in FMF

patients, which require further studies. Understanding of the mechanism underlying this, may lead to explanation pathogenesis of FMF disease.

We were confirmed the bioinformatic analysis, carrying out PCR with MEFV primers specific to predetected peak region in MEFV and primers of randomly selected genes which are TNFSRF1A and NLRP3 using the same ChIP enriched DNA samples, since amplification of the H3K9me3 and H3K4me3 in these regions was observed. Also we used additional controls which are positive control primers, negative control primers and no template control in standart PCR. In our experiment, positive control for active transcriptional states of chromatin (H3K4me3) is a negative control for repressed chromatin (H3K9me3) and *vice versa.* Furthermore, PCR was performed in individual samples that 3 of FMF patients during attack, the same FMF patients during attack free period and healthy subjects. Regarding our PCR experiment, it couldn't be normalized enrichment of H3K4me3 mark in FMF patients during attack period according to other mark and study groups because of lower amount of DNA, not sensitive PCR, specifity of primers, intensity, resolution differences and level of background signal. PCR using negative control primer and negative control IgG was generated product resulting from non-spesific with high level background. Not sheared chromatin, too much antibody, too much DNA in PCR reaction, poor washing, unblocked magnetic beads, primer specifity may increase background.

For further studies, a larger number of patients and control sapmles are needed for statistical analysis and validation of the ChIP experiment. ChIP should be coupled with high throughput sequencing with deeper coverage in order to deeper genome wide analysis of the histone modifications. Also, ChIP-Seq data confirmed using quantitative real time PCR.

REFERENCES

Auclair, G. and Weber, M. (2012). Mechanisms of DNA methylation and demethylation in mammals. *Biochimie*, **94**, 2202-2211.

Ahmadinejad, Z., Mansori, S., Ziaee, V., Alijani, N., Aghighi, Y., Parvaneh, N. and Mordinejad, H. M. (2014). Periodic Fever: A Review on Clinical, Management and Guideline for Iranian Patients - Part I. *Iran J Pediatr*., **24**, 1, 1-13.

Akpolat, T., Özkaya, O., Özen, S. (2012). Homozygous M694V as a risk factor for amyloidosis in Turkish FMF patients. *Gene,* **492**, 285–289.

Aksentijevich, I. and Kastner L. D. (2011). Genetics of monogenic autoinflammatory diseases: past successes, future challenges. *Nature Reviews Rheumatology*, **7**, 469-478 doi:10.1038/nrrheum.2011.94.

Bailey, T., Krajewski, P., Ladunga, I., Lefebvre, C., Li, Q., Liu, T., Madrigal, P., Taslim, C., Zhang, J. (2013). Practical Guidelines for the Comprehensive Analysis of ChIP-Seq Data. *PLOS Computational Biology*, **9**, 11.

Barski, A., Cuddapah, S., Cui, K., Roh, T. Y., Schones, D. E., Wang, Z., Wei, G., Chepelev, I. and Zhao, K. (2007). High-resolution profiling of histone methylations in the human genome. *Cell*, **129**, 823-37.

Barozzi, I., Termanini, A., Minucci, S. and Natoli, G. (2011). Fish the ChIPs: a pipeline for automated genomic annotation of ChIP-Seq data. *Biology Direct*, **6**, 51.

Beckmann, J. S. and Trifonov, E. N. (1991). Biochemistry Splice junctions follow a 205-base ladder (intron/exon/chromatin/higher order structure). *Proc. Natl. Acad. Sci. USA*, **88**, 2380-2383.

Ben-Zvi, I., Brandt, B., Berkun, Y., Lidar , M., Livneh, A. (2012). The relative contribution of environmental and genetic factors to phenotypic variation in familial Mediterranean fever (FMF). *Gene*, **491**, 260–263.

Ben-Zvi, I., Herskovizh, C., Kukuy, O., Kassel, Y., Grossman, C. and Livneh, A. (2015). Familial Mediterranean fever without MEFV mutations: a case–control study. *Orphanet Journal of Rare Diseases*, **10**, 34.

Berkun, Y., Levy, R., Hurwitz, A., Meir-Harel, M., Lidar, M., Livneh, A., and Padeh, S. (2011). The Familial Mediterranean Fever Gene as a Modifier of Periodic Fever, Aphthous, Stomatitis, Pharyngitis, and Adenopathy Syndrome. *Semin Arthritis Rheum*, **40**, 467-472.

Bernot, A., Clepet, C., Dasilva, C., Devaud, C., Petit, J. L., Caloustian, C. et al. (1997). A candidate gene for familial Mediterranean fever. *Nat Genet*., **17**, 1, 25-31.

Bird, A. (2002). DNA methylation patterns and epigenetic memory. *Genes and Development,*, **16**, 6–21.

Brinkman, B. A., Gu, H., Bartels, J. S., Zhang, Y., Matarese, F., Simmer, F. et al. (2012). Sequential ChIP-bisulfite sequencing enables direct genome-scale investigation of chromatin and DNA methylation cross-talk. *Cold Spring Harbor Laboratory Press*, **22**, 1128–1138.

Bonyadi, J. M., Gerami, N. M. S., Somi, H. M., and Dastgiri, S. (2015). *MEFV* mutations in Northwest of Iran: a cross sectional study. Iran J Basic Med Sci., **18**, 1, 53–57.

Booty, G. M., Chae, J. J., Masters, L. S., Remmers, F. E., Barham, B., Le, M. J. et al. (2009). Familial Mediterranean Fever With a Single *MEFV* Mutation. *Arthritis and Rheumatism*, **60**, 6, 1851–1861.

Cattan, D., Notarnicola, C., Molinari, N. and Touitou, I. (2000). Inflammatory bowel disease in non-Ashkenazi Jews with familialMediterranean fever. *Lancet*, **355**, 378–379.

Centola, M., Wood, G., Frucht, M. D., Galon, J., Aringer, M., Farrell, C., et al. (2000). The gene for familial Mediterranean fever, *MEFV*, is expressed in early leukocyte development and is regulated in response to inflammatory mediators. *Blood*, **95**, 10.

Chae, J. J., Aksentijevich, I. and Kastner, L. D. (2009). Advances in the understanding of familial Mediterranean fever and possibilities for targeted therapy. *British Journal of Haematology*, **146**, 467–478.

Chen, K., Dai, X. and Wu, J. (2015). Alternative splicing: An important mechanism in stem cell biology. *World J Stem Cells*, **7**, 1, 1-10.

Chojnowski, K., Goryca, K., Rubel, T. and Mikula, M. (2014). jChIP: a graphical environment for exploratory ChIP-Seq data analysis. *BMC Research Notes*, **7**, 676.

Choy, S. J., Wei, S., Lee, Y. J., Chu, S., Tan, S. and Lee, H. T. (2010). DNA Methylation Increases Nucleosome Compaction and Rigidity. *J Am Chem Soc*., **132**, 6, 1782–1783.

Cosan, F., Üstek, D., Oku, B., Duymaz-Tozkir, J., Cakiris, A., Abaci, N. et al. (2010). Association of Familial Mediterranean Fever–Related MEFV variations With Ankylosing Spondylitis. *Arthritis and Rheumatism*, **62**, 11, 3232-3236.

De Jesus, A. A. and Mansky, G. R. (2013). Monogenic Autoinflammatory Diseases: Concept And Clinical Manifestations. *Clin Immunol.*, **147**, 3, 155–174.

Diaz, A., Hu, C., Kastner, L. D., Schaner, P., Reginato, M. A., Richards, N. and Gumucio, L. D. (2004). Lipopolysaccharide-Induced Expression of Multiple Alternatively Spliced *MEFV* Transcripts in Human Synovial Fibroblasts: a prominent splice isoform lacks the C-terminal domain that is highly mutated in familial Mediterranean fever. *Arthritis Rheum.*,**50**, 11, 3679–3689.

Di Lorenzo, A. and Bedford, M. T. (2011). Histone arginine methylation. *FEBS Lett*, **585**, 2024-2031.

Dov, B. C., Hartmann, B., Lundgren, J. and Valca´rcel, J. (2008). Genome-wide Analysis of Alternative Pre-mRNA Splicing. *The Journal of Biological Chemistry*, **283**, 3, 1229–1233.

Ece, A., Cakmak, E., Uluca, U., Kelekci, S., Yolbas¸ I., Gunes¸ A., Yel, S., Tan, I., Sen, V. (2014). The MEFV mutations and their clinical correlations in children with familial Mediterranean fever in southeast Turkey. *Rheumatol Int*, **34**, 207–212.

Espada, J., Ballestar, E., Fraga, F. M., Garea, V. A., Juarranz, A., Stockert, C.J., Robertson, D. K., Fuks, F. and Etseller, M. (2004). Human DNA Methyltransferase 1 Is Required for Maintenance of the Histone H3 Modification Pattern. *J. Biol. Chem.*, ***279****, 37175-37184.*

Federici, S., Caorsi, R. and Gattorno, M. (2012). The autoinflammatory diseases. *Swiss Med Wkly.*, **142**, 1-17.

Feng, J., Liu, T., Qin, B., Zhang, Y. and Liu, S. X. (2012). Identifying ChIP-Seq enrichment using MACS. *Nature Protocols*, **7**, 9.

Fidder, H., Chowers, Y., Ackerman, Z., Pollak, R. D., Crusius, J. B., Livneh, A., Bar-Meir, S., Avidan, B. and Shinhar, Y. (2005). The familial Mediterranean fever (MEVF) gene as a modifier of Crohn's disease. *Am J Gastroenterol.*, **100**, 2, 338-343.

Fuks, F., Hurd, J. P., Deplus, R. and Kouzarides, T. (2003). The DNA methyltransferases associate with HP1 and the SUV39H1 histone methyltransferase. *Nucleic Acids Research*, **31**, 9, 2305-2312.

Fulwood, M. J. and Ruan, Y. (2009). ChIP-based methods for the identification of long-range chromatin interactions. *J Cell Biochem*, **107**, 30-9.

Galon, J., Aksentijevich, I., McDermott, F. M., O'Shea, J. J, and Kastner, L. D. (2000). *TNFRSF1A* mutations and autoinflammatory syndromes. *Current Opinion in Immunology*, **12**, 479–486.

Gilmour, D. S. and Lis, J. T. (1984). Detecting protein-DNA interactions in vivo: Distribution of RNA polymerase on specific bacterial genes. Proc. *Natl. Acad. Sci*., **81**, 4275-4279.

Gilmour, D. S. and Lis, J. T. (1985). In vivo interactions of RNA polymerase II with genes of Drosophila melanogaster. *Mol. Cell Biol.*, **5**, 2009–2018.

Gilmour, D. S. and Lis, J. T. (1986). RNA polymerase II interacts with the promoter region of the noninduced hsp70 gene in Drosophila melanogaster cells. *Mol. Cell Biol*., **6**, 3984–3989.

Grandemange S., Soler S. and Touitou I. (2009). Expression of the familial Mediterranean fever gene is regulated by nonsense-mediated decay. *Human Molecular Genetics*, **18**, 24, 4746–4755.

Guenther, M. G., Levine, S. S., Boyer, L. A., Jaenisch, R. and Young, R. A. (2007). A chromatin landmark and transcription initiation at most promoters in human cells. *Cell*, **130**, 77- 88.

Guo, U. J, Su, Y., Zhong, C., Ming, G. and Song, H. (2011). Hydroxylation of 5-methylcytosine by TET1 promotes active DNA demethylation in the adult brain. *Cell*, **145**, 3, 423–434.

Handy, E. D., Castro, R. and Loscalzo, J. (2011). Epigenetic Modifications: Basic Mechanisms and Role in Cardiovascular Disease. *Circulation*, **123**, 19, 2145–2156.

Hashim M. M., Nehme, N., Chouery, E., Jalkh, N. and Megarbane, A. (2010). 1Novel *MEFV* transcripts in Familial Mediterranean fever patients and controls. *BMC Medical Genetics*, **11**, 87.

Hashimoto, H., Vertino, M. P. and Cheng, X. (2010). Molecular coupling of DNA methylation and histone methylation. *Epigenomics*, **2**, 5, 657–669.

Hashimshony T., Zhang, J., Keshet, I., Bustin, M. and Cedar, H. (2003). The role of DNA methylation in setting up chromatin structure during development. *Nat Genet*, **34**, 187-92.

Haring, M., Offermann, S., Danker, T., Horst, I., Peterhansel, C. and Stam, M. (2007). Chromatin immunoprecipitation: optimization, quantitative analysis and data normalization. *Plant Method*, **3**, 11.

Heintzman, N. D., Hon, G. C., Hawkins, R. D., Kheradpour, P., Stark, A., Harp, L. F. et al. (2009). Histone modifications at human enhancers reflect global cell-type-specific gene expression. *Nature*, **459**, 108-112.

Hermann, A., Schmitt, S. and Albert Jeltsch, A. (2003). The Human Dnmt2 Has Residual DNA-(Cytosine-C5) Methyltransferase Activity. *The Journal of Biological Chemistry*, **278**, 34, 31717–31721.

Hodges, C., Bintu, L., Lubkowska, L., Kashlev, M. And Bustamante, C. (2009). Nucleosomal Fluctuations Govern the Transcription Dynamics of RNA Polymerase II. *Science*, **325**, 5940, 626–628.

Horsburgh, S., Robson-Ansley, R., Adams, R. and Smith, C. (2015). Exercise and inflammation-related epigenetic modifications: focus on Dna methylation. *Exerc Immunol Rev*., **21**, 26-41.

Hu, L. J., Zhoua, O. B., Zhanga, R. R., Zhangc, L. K., Zhoua, Q. J. and Xua, L. G. (2009). The N-terminus of histone H3 is required for de novo DNA methylation in chromatin. *Pnas*, **106**, 52, 22187–22192.

Huh,I., Zeng, J., Park, T. and Yi, V. S. (2013). DNA methylation and transcriptional noise. *Epigenetics & Chromatin*, **6**, 9.

Jia, D., Jurkowska, Z. R., Zhang, X., Jeltsch, A. and Cheng, X. (2007). Structure of Dnmt3a bound to Dnmt3L suggests a model for *de novo* DNA methylation. *Nature*, **449**, 7159, 248–251.

Jiang, Y., Bressler, J. and Beaudet, L. A. (2004). Epigenetics and Human disease. *Annu. Rev. Genomics Hum. Genet*., **5**, 479–510.

Jones, P. L., Veenstra, G. J., Wade, P. A., Vermaak, D., Kass, S. U. et al. (1998). Methylated DNA and MeCP2 recruit histone deacetylase to repress transcription. *Nat Genet.*, **19**, 2,187-91.

Kanherkar, R. R., Bhatia-Dey, N. and Csoka, B. A. (2014). Epigenetics across the human lifespan. *Frontiers in Cell and Developmental Biology*, **2**, 49.

Karpen, G. H. and Allshire, R. C. (1997). The case for epigenetic effects on centromere identity and function. *Trends Genet*, **13**, 489-496.

Kass, S. U., Landsberger, N. and Wolffe, A. P. (1997). DNA methylation directs a timedependent repression of transcription initiation. *Curr Biol*, **7**,157-165.

Kirectepe, K. A., Erdem, C. G., Senturk, N., Arisoy, N., Hatemi, G., Ozdogan, H., Kasapcopur, O., Turanli, T. E. (2011). Increased expression of exon 2 deleted MEFV transcript in familial Mediterranean fever patients. *International Journal of Immunogenetics*, **38**, 327–329.

Kirectepe, K. A., Kasapcopur, O., Arisoy, N., Erdem, Ç. G., Hatemi, G., Ozdogan, H. and Turanli, T. E. (2011). Analysis of MEFV exon methylation and expression patterns in familial Mediterranean fever. *BMC Medical Genetics*, **12**, 105.

Kohli, M. R. and Zhang, Y. (2013). TET enzymes, TDG and the dynamics of DNA demethylation. *Nature*, **502**, 7472, 472–479.

Koorosh, K. (2012). Epigenetic programming defines stem cell identity and entry into the proliferative compartment in chronic myeloid leukaemia *(CML).* (PhD thesis) http://theses.gla.ac.uk/3929/.

Kouzarides, T. (2007). Chromatin Modifications and Their Function. *Cell*, **128**, 693–705.

Krig, R. S., Jin, X. V., Bieda, C. M., O'Geen, H., Yaswen, P., et al. (2007). Identification of genes directly regulated by the oncogene ZNF217 using ChIP-chip assays. *J Biol Chem.*, **282**, 13, 9703–9712.

Landt, G. S., Marinov, K. G., Kundaje, A., Kheradpour, P., Pauli, F., Batzoglou, S. et al. (2012). ChIP-Seq guidelines and practices of the ENCODE and modENCODE consortia. *Cold Spring Harbor Laboratory Press*, **22**, 1813–1831.

Laurent, L., Wong, E., Li, G., Huynh, T., Tsirigos, A., Ong, T. C. et al. (2010). Dynamic changes in the human methylome during differentiation. *Cold Spring Harbor Laboratory Press*, **20**, 320–331.

Li, B., Carey, M. and Workman, L. J. (2007). The Role of Chromatin during Transcription. *Cell*, **128**, 707–719.

Li, Z. B., Huang, Z., Cui, Y. Q., Song, H. X., Du, L., Jeltsch, A. et al. (2011). Histone tails regulate DNA methylation by allosterically activating *de novo* methyltransferase. *Cell Research*, **21**, 1172-1181.

Liu, T. E., Pott, S. and Huss, M. (2010). Q&A: ChIP-Seq technologies and the study of gene regulation. *BMC Biology*, **8**, 56.

Liu, H., Jin, T., Guan, J. and Zhou, S. (2014). Histone modifications involved in cassette exon inclusions: a quantitative and interpretable analysis. *BMC Genomics*, **15**, 1148, 1-13.

Livneh, A., Aksentijevich, I., Langevitz, P., Torosyan, Y. et al. (2001). A single mutated MEFV allele in Israeli patients suffering from familial Mediterranean fever and Behcet's disease (FMF-BD). *European Journal of Human Genetics*, 9, 191–196.

Liyanage, B. R. V., Jarmasz, S. J., Murugeshan, N., Del Bigio, R. M., Rastegar, M. and Davie R. J. (2010). DNA Modifications: Function and Applications in Normal and Disease States. *Biology*, **3**, 670-723.

Luger, K., Mader, W. A., Richmond, K. R., Sargent, R. D. and Richmond, J. T. (1997). Crystal structure of the nucleosome core particle at 2.8Å resolution. *Nature*, **389**, 251-260.

Matzner, Y., Abedat, S., Shapiro, E., Eisenberg, S. et al. (2010). Expression of the familial Mediterranean fever gene and activity of the C5a inhibitor in human primary fibroblast cultures. *Blood*, **96**, 2.

Meissner, A., Mikkelsen, T. S., Gu, H., Wernig, M., Hanna, J., Sivachenko, A. et al. (2008). Genome-scale DNA methylation maps of pluripotent and differentiated cells. *Nature*, **454**, 766-70.

Menthie`re, S. C., Terrie`re, S., Pugne`re, D., Ruiz, M., Demaille, J. and Touitou, I. et al. (2003). INFEVERS: the Registry for FMF and hereditary inflammatory disorders mutations. *Nucleic Acids Research*, **31**, 1, 282–285.

Mikkelsen, T. S., Ku, M., Jaffe, D. B., Issac, B., Lieberman, E., Giannoukos, G. et al. (2007). Genome-wide maps of chromatin state in pluripotent and lineage-committed cells. *Nature*, **448**, 553-60.

Mukhopadhyay, A., Deplancke, B., Walhout, M. J. A. and Tissenbaum, A. H. (2008). Chromatin immunoprecipitation (ChIP) coupled to detection by quantitative real-time PCR to study transcription factor binding to DNA in *Caenorhabditis elegans. Nat Protoc.*, **3**, 4, 698–709.

Nan, X., Ng, H. H., Johnson, C. A., Laherty, C. D., Turner, B. M., Eisenman, R. N., Bird, A. (1998). Transcriptional repression by the methyl-CpG-binding protein MeCP2 involves a histone deacetylase complex. *Nature.*, **28**, 393(6683), 386-389.

Notarnicola, C., Didelot, N. M., Paut, K. I., Seguret, F., Demaille, J. and Touitou, I. (2002). Reduced MEFV Messenger RNA Expression in Patients With Familial Mediterranean Fever. *Arthritis and Rheumatism*, **46**, 10, 2785–2793.

Okano, M., Xie, S. and Li, E. (1998). Dnmt2 is not required for de novo and maintenance methylation of viral DNA in embryonic stem cells. *Nucleic Acids Research*, **26**, 11, 2536–2540.

O'neill, L. P. and Turner, B. M. (1996). Immunoprecipitation of chromatin. *Methods Enzymol*, **274**, 189-197.

O'neill, L. P. and Turner, B. M. (2003). Immunoprecipitation of native chromatin: NChIP. *Methods*, **31**, 76-82.

Ooi, S. K., Qiu, C., Bernstein, E., Li, K., Jia, D., Yang, Z. et al. (2007). DNMT3L connects unmethylated lysine 4 of histone H3 to de novo methylation of DNA. *Nature*, **448**, 714-717.

Orlando, V., Strutt, H. and Paro, R. (1997). Analysis of chromatin structure by in vivo formaldehyde cross-linking. *Methods*, **11**, 205-214.

Orphanides, G. and Reinberg, D. (2000). RNA polymerase II elongation through chromatin. *Nature*, **407**, 471-475.

Ozkurede, U. V. and Franchi, L. (2012). Immunology in clinic review series; focus on autoinflammatory diseases: role of inflammasomes in autoinflammatory syndromes. *Clin Exp Immunol.*, **167**, 3, 382–390.

Bortz, S. D. P., and Wamhoff, R. B. (2011). Chromatin Immunoprecipitation (ChIP): Revisiting the Efficacy of Sample Preparation, Sonication, Quantification of Sheared DNA, and Analysis via PCR. *PLoS ONE*, **6**, 10.

Pan, G., Tian, S., Nie, J., Yang, C., Ruotti, V., Wei, H. et al. (2007). Whole-Genome Analysis of Histone H3 Lysine 4 and Lysine 27 Methylation in Human Embryonic Stem Cells. *Cell Stem Cell*, **1**, 299–312.

Park, J. P. (2009). ChIP-Seq: advantages and challenges of a maturing technology. *Nat Rev Genet.*, **10**, 10, 669–680.

Pepke, S., Wold, B. and Mortazavi, A. (2009). Computation for ChIP-Seq and RNA-seq studies. *Nature Methods*, **6**, 11 0, 22–32.

Peynircioğlu, B. and Yılmaz, E. (2006). Ailevi akdeniz ateşi hastalığının moleküler temeli. *Hacettepe Tıp Dergisi*, **37**, 223-229.

Pichler, G., Wolf, P., Schmidt, S. C., Meilinger, D., Schneider, K., Frauer, C. et al. (2011). Cooperative DNA and Histone Binding by Uhrf2 Links the Two Major Repressive Epigenetic Pathways. *Journal of Cellular Biochemistry*, **112**, 2585–2593.

Podlaha, O., De, S., Gonen, M., Michor, F. (2014). Histone Modifications Are Associated with Transcript Isoform Diversity in Normal and Cancer Cells. *PLOS Computational Biolog*, **10**, 6.

Pomraning, R. K., Smith, M. K., Freitag, M. (2009). Genome-wide high throughput analysis of DNA methylation in eukaryotes. *Methods*, **47**, 142–150.

Ronderos, Q. P. and Ortiz, M. G. (2011). Epigenetics and Autoimmune Diseases. *Autoimmune Diseases*, **2012**, 1-16.

Rosenfeld, A. J., Wang, Z., Schones, E. D., Zhao, K., DeSalle, R. and Zhang, Q. Z. (2009). Determination of enriched histone modifications in non-genic portions of the human genome. *BMC Genomics*, **10**, 143.

Rose, R. N. and Klose J. R. (2014). Understanding the relationship between DNA methylation and histone lysine methylation. *Biochim. Biophys. Acta*, **670**, 1-11.

Rothbart, B. S., Krajewski, K., Nady, N., Tempel, W., Xue, S., Badeaux, I. A. et al. (2012). Association of UHRF1 with methylated H3K9 directs the maintenance of DNA methylation. ***Nature Structural and Molecular Biology***, **19**, 11, 1155-1162.

Saksouk, N., Simboeck, E. and Déjardin, J. (2015). Constitutive heterochromatin formation and transcription in mammals. *Epigenetics and Chromatin*, **8**, 3.

Schmid, D. C. and Bucher, P. (2007). ChIP-Seq Data Reveal Nucleosome Architecture of Human Promoters. *Cell*, **131**, 5, 831-832.

Seo, J. Y., Park, J. Y., Yi, A. Y., Hwang, Y. J., Lee, B. I., Cho, H. B. et al. (2014). Epigenetics: general characteristics and implications for oral health. *RDE*, **40**, 1, 14-22.

Sims, J. R., Millhouse, S., Chen, F. C., Lewis, A. B., Bromage, E. H. et al. (2007). Recognition of Trimethylated Histone H3 Lysine 4 Facilitates the Recruitment of Transcription Post-Initiation Factors and premRNA Splicing. *Mol Cell*, **28**, 44, 665–676.

Solomon, M. J., Larsen, P.L., Varshavsky, A. (1988). Mapping protein- DNA interactions in vivo with formaldehyde: Evidence that histone H4 is retained on a highly transcribed gene. *Cell*, **53,** 937–947.

Solomon, M. J. and Varshavsky, A. (1985). Formaldehyde-mediated DNA-protein crosslinking: a probe for in vivo chromatin structures. *Proc Natl Acad Sci USA*, **82**, 6470-6474.

Soriano, A. and Pras, E. (2014). Familial Mediterranean Fever: Genetic Update. *Imaj*, **16**, 274-276.

Storey, J. D. and Tibshirani, R. (2003). Statistical significance for genomewide studies. *Proc Natl Acad Sci USA*, **100**, 9440-9445.

Squazzo, L. S., O'Geen, H., Komashko, M. V., Krig, R. S., Jin, X. V., Jang, S. et al. (2006). Suz12 binds to silenced regions of the genome in a cell-type-specific manner. *Cold Spring Harbor Laboratory Pres*, **16**, 890–900.

Taskiran, Z. E., Cetinkaya, A., Peynircioglu, B. B., Akkaya, Z. Y. and Yilmaz E. (2012). The Effect of Colchicine on Pyrin and Pyrin Interacting Proteins. *Journal of Cellular Biochemistry*, **113**, 3536–3546.

The International FMF Consortium (1997). Ancient Missense Mutations in a New Member of the *RoRet* Gene Family Are Likely to Cause Familial Mediterranean Fever. *Cell*, **90**, 797–807.

Touitou, I. (2001). The spectrum of Familial Mediterranean Fever (FMF) mutations. *European Journal of Human Genetics*, **9**, 473-483.

Üstek, D., Ekmekçi, G. C., Selçukbiricik, F., Cakiris, A., Oku, B., Vural, B. et al. (2007). Association Between Reduced Levels of *MEFV* Messenger RNA in Peripheral Blood Leukocytes and Acute Inflammation. *Arthritis and Rheumatism*, **56**, 1, 345–350.

Warrier, A. R. (2010). Writers and readers of histone H3 methylation. *Open Access*, PhD Thesis.

Venolia, L. and Gartler, S. M. (1983). Comparison of transformation efficiency of human active and inactive X-chromosomal DNA. *Nature*, **302**, 82-83.

Verdone, L., Agricola, E., Caserta, M. and Di Mauro, E. (2006). Histone acetylation in gene regulation. *Briefings in Functional Genomics and Proteomics*, **5**, 3, 209-221.

Villeneuve, M. L., Reddy, A. M., Lanting, L. L., Wang, M., Meng, L. and Natarajan, R. (2008). Epigenetic histone H3 lysine 9 methylation in metabolic memory and inflammatory phenotype of vascular smooth muscle cells in diabetes. *Pnas*, **105**, 26, 9047–9052.

Wells, J. and Farnham, P. J. (2002). Characterizing transcription factor binding sites using formaldehyde crosslinking and immunoprecipitation. *Methods*, **26**, 48-56.

Wilson, G. A. (2008). Epigenetic Regulation of Gene Expression in the Inflammatory Response and Relevance to Common Diseases. *J Periodontol*, **79**, 1514-1519.

Xu, S., Grullon, S., Ge, K. and Peng, W. (2014). Spatial Clustering for Identification of ChIP-Enriched Regions (SICER) to Map Regions of Histone Methylation Patterns in Embryonic Stem Cells. *Methods Mol Biol.*, **1150**, 97–111.

Yamaguchi, N., Winter, M. C., Wu, F. M., Kwon, S. C., William, A. D. and Wagnera, D. (2014). Chromatin Immunoprecipitation from Arabidopsis Tissues. *The Arabidopsis Book*, 1-9 doi: 10.1199/tab.0170.

Yan, H., Evans, J., Kalmbach, M., Moore, R., Middha, S., Luban, S. et al. (2014). HiChIP: a high-throughput pipeline for integrative analysis of ChIP-Seq data. *BMC Bioinformatics*, **15**, 280.

Zeng, W., Greef, C. J., Chen, Y., Chien, R., Kong, X., Gregson, C. H. et al. (2009). Specific Loss of Histone H3 Lysine 9 Trimethylation and HP1c/Cohesin Binding at D4Z4 Repeats Is Associated with Facioscapulohumeral Dystrophy (FSHD). *PLoS Genetics*, **5**, 7.

APPENDICES

APPENDIX A : Laboratory Equipment
APPENDIX B : Chemicals, Enzymes, Markers and Commercial Kits
APPENDIX C : Preparation of Buffers
APPENDIX D : Bioinformatic Analysis

APPENDIX A

Table A.1: Laboratory equipment.

Centrifuges	Thermo Scientific MICROCL 17 Allegra 25R Centrifuge Beckman Coulter Beckman Coulter Microfuge®18
Centrifuge Tubes	Greiner Bio-One Axygen
Pipette Tips	Axygen and Thermo Scientific
Pipettes	Axygen and Thermo Scientific
Vortex	Herdolph Reax Top
Heat Block	Dri-Block® DB-2D- Bibby Scientific Ltd
pH Meter	Mettler Toledo MP220
Spectrophotometer	NANODROP- Thermo Scientific
Examination Gloves	Beybi
Electrophoresis Systems	BIO-RAD Mini-PROTEAN® Tetra Cell
Transfer System	BIO-RAD Trans-Blot Turbo Transfer
Light Microscope	Olympus CH30
Hemacytometer	FisherLab Scientific, 0267110
High Pressure Steam Sterilizer	TOMY SX-700E
Ice Machine	Scotsman AF 10
Freezers	Vestel (+4^{o}C) Arçelik (-20^{o}C) Nuve (-80^{o}C)
Kodak Medical X-ray Processor	Kodak
Magnetic Separator	Promega
Microwave	Arcelik MD582
Rotator	Stuart
Syringe Filtre	TPP 0,22 μm
Serological Pipette	Greiner bio-one CELLSTAR® 5, 10, 25 mL
Sonicator	Bandelin Sonoplus
Shaker	Heidolph Doumax 1030

APPENDIX B

Table B.1: Chemicals.

Acetic Acid	Riedel-de Haën
Acrylamide/Bis Solution	BIO-RAD
Agarose	AppliChem
Ammonium persulphates	Sigma Aldrich
EDTA	AppliChem
EtBr	Amresco
Ethanol	Sigma Aldrich
Dynal Protein G beads	Life Technologies
Dynal Protein A beads	Life Technologies
dNTP Mix	Thermo Scientific
Glycine	AppliChem
HCl	AppliChem
Histopaque-1077	Sigma-Aldrich
NaCl	Fluka
Phosphate Buffered Saline	Sigma Aldrich
Primers	Alpha DNA
RPMI	LONZA
Q5 PCR Buffer	New England BioLabs
Sodium Dodecyl Sulfate	AppliChem
TEMED	AppliChem
Tris	AppliChem
Triton X-100	Merck
Trypan blue	Sigma Aldrich
Tween-20	AppliChem
6X Loading Dye	Fermentas

Table B.2: Enzymes.

Proteinase K	Ambion
RNase A	Roche
Complete EDTA-free Protease Inhibitor Cocktail II	Roche
SYBR®-Green Master Mix	Life Technologies
Q5® Hot Start High-Fidelty DNA Polymerase	New England BioLabs

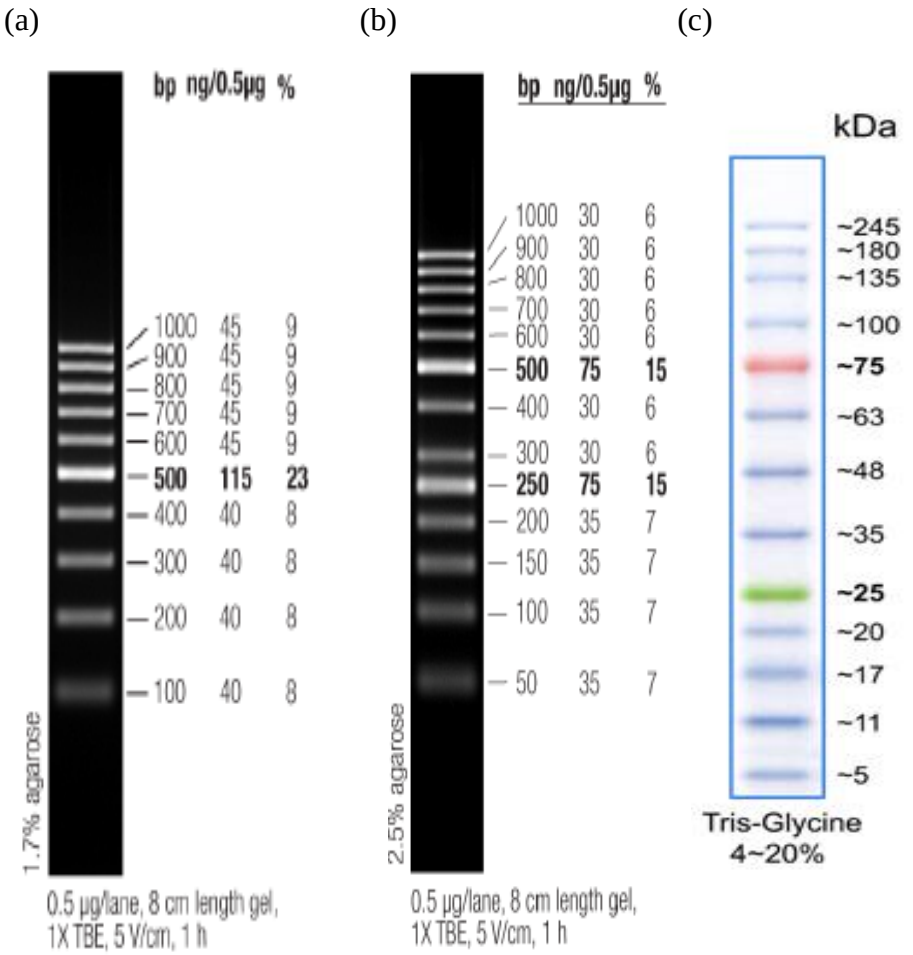

Figure B.1: Markers. (a) Gene Ruler 100 bp DNA Ladder (Fermentas). (b) Gene Ruler 50 bp DNA Ladder (Fermentas). (c) BLUelf Prestained Protein Ladder (GeneDirex).

Table B.3: Commercial Kits.

ChIP DNA Clean & Concentrator	Zymo Research
Western Blot Kit	BioRad

APPENDIX C

Table C.1: ChIP lysis buffer.

	Concentration
HEPES	50 mM
NaCI	150 mM
Triton X-100	%1
Na-deoxycholate	%0.1
EDTA	1 mM
SDS	%1
dH_2O	Add to 500 mL

Table C.2: Elution buffer.

	Concentration
SDS	%20
NaHCO3	1 M
dH_2O	Add to 2 mL

Table C.3: Glycine buffer.

	Concentration
Glycine	1.25 M
dH_2O	Add to 25 mL

Table C.4: High salt ChIP lysis buffer.

	Concentration
HEPES	50 mM
NaCI	500 mM
Triton X-100	%1
Na-deoxycholate	%0.1
EDTA	1 mM
dH2O	Add to 500 mL

Table C 5: Low salt ChIP lysis buffer.

	Concentration
HEPES	50 mM
NaCI	150 mM
Triton X-100	%1
Na-deoxycholate	%0.1
EDTA	1 mM
dH_2O	Add to 500 mL

Table C.6: SDS-polyacrylamide gel.

4% Stacking Gel	
Acrylamide/Bis-acrylamide	0.67 mL
20% SDS	0.025 mL
0.5 M Tris-HCL, pH 6.8	1.25 mL
dH_2O	3.075 mL
10% APS	0.025 mL
TEMED	0.005 mL
12% Separating Gel	
Acrylamide/Bis-acrylamide	4 mL
20% SDS	0.05 mL
1.5 M Tris-HCL, pH 8.8	2.5 mL
dH_2O	3.4 mL
10% APS	0.05 mL
TEMED	0.005 mL

Table C.7: TAE buffer.

	Concentration
Tris-base	24.2 g
Acetic Acid	5.71 mL
EDTA	25.4 mL
dH_2O	Add to 500 mL

Table C.8: TE buffer.

	Concentration
Tris	10 mM
EDTA	1 mM
dH_2O	Add to 1 L

Table C.9: PBS-T.

	Concentration
PBS	1X
Tween-20	%0.02
dH_2O	Add to 250 mL

APPENDIX D

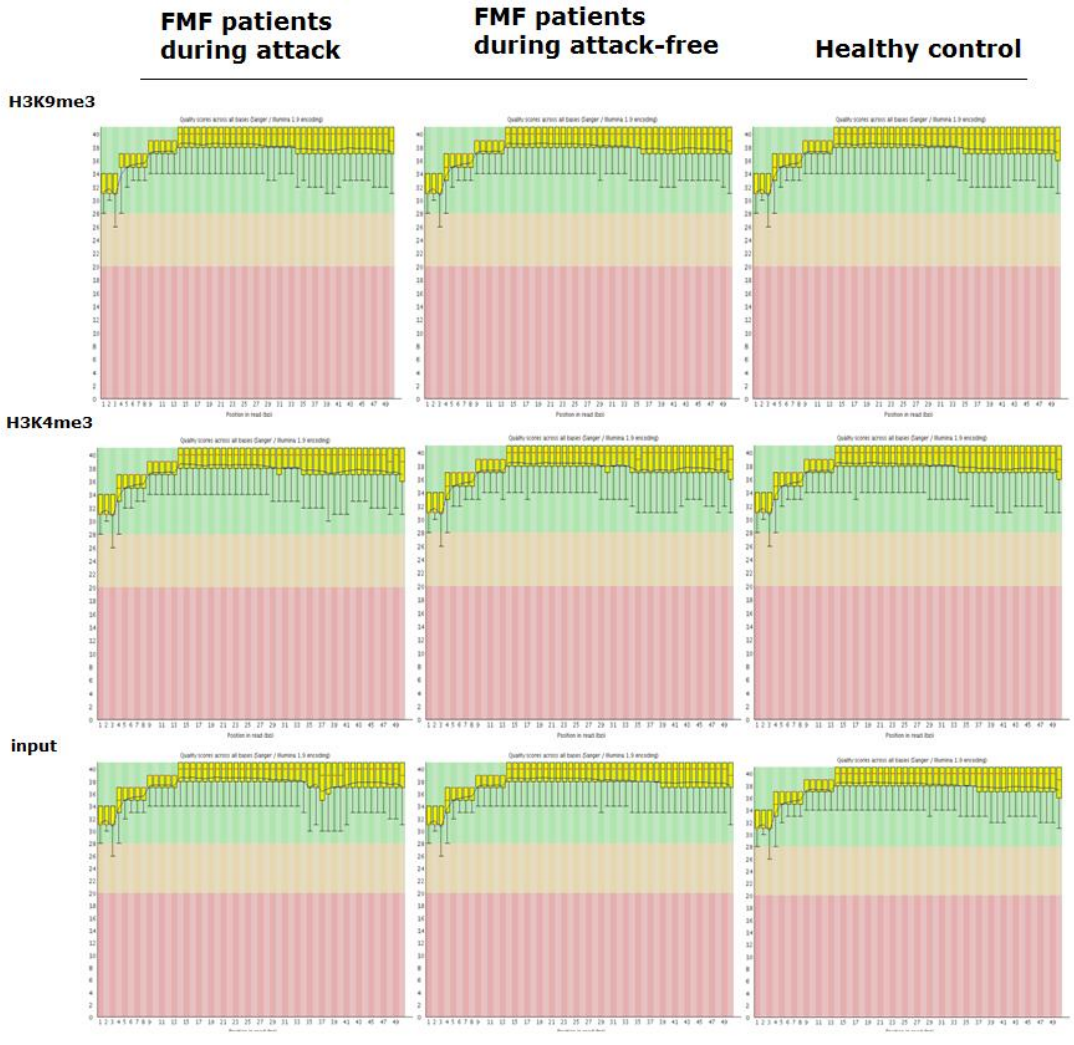

Figure D.1: FASTQC per base quality report.

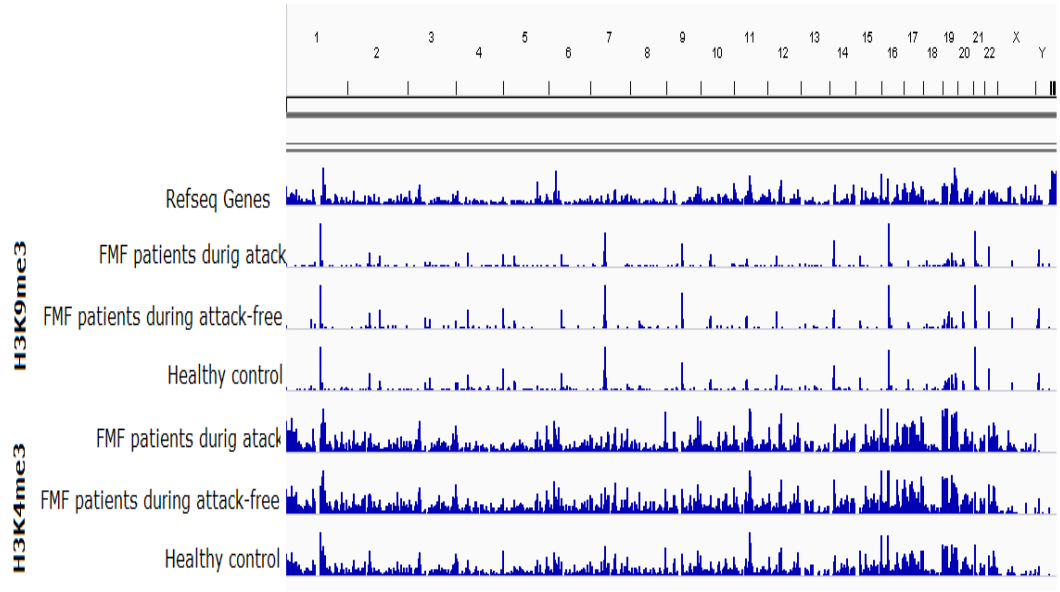

Figure D.2: ChIP-Seq peaks genome wide localizations.

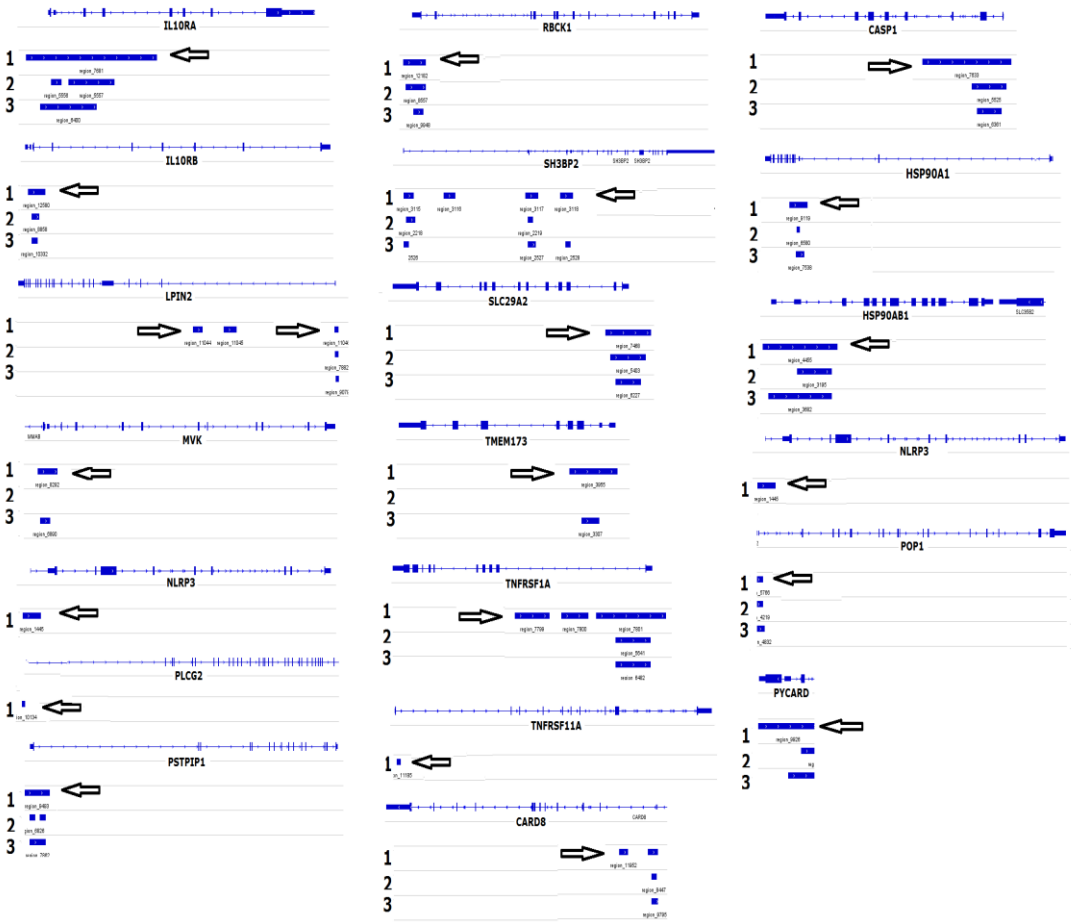

Figure D.3: H3K4me3 peaks on the candidate genes. (1: FMF patients during attack, 2: FMF patients during attack-free, 3: Healthy control).

CURRICULUM VITAE

Name Surname:	Begüm FİDAN
Place and Date of Birth:	Bakırköy/İstanbul 27.10.1989
E-Mail:	begum_fidan@windowslive.com
B.Sc.:	2006-2010: Marmara University- Faculty of Art and Science- Biology, Turkey
M.Sc.:	2011-2015: Istanbul Technical University- Molecular Biology Genetics and Biotechnology, Turkey
Certificates:	2006-2010: Marmara University (Minor)- Faculty of Art and Science- Chemistry, Turkey
	2006-2010: Marmara University (Pedagogy)- Faculty of Art and Science- Biology,Turkey

Publications, Presentations And Patents On The Thesis:

B. Fidan, I. Karacan, H. Ozdogan, S. Ugurlu, E. Seyahi, E. Tahir Turanli (2015). *Analysis of Histone Modification in Familial Mediterranean Fever Patients*. The European Human Genetics Conference 2015, 6-9 June, Glasgow, Scotland, UK.